



# Numerical Weather Prediction

Methods of improving the representation of ozone in the Met Office Model



Forecasting Research Technical Report No. 502

Author(s): Camilla Mathison, David R. Jackson and Mike Keil

*email: [nwp\\_publications@metoffice.gov.uk](mailto:nwp_publications@metoffice.gov.uk)*

©Crown Copyright

---

# Forecasting Research Technical Report No. 502

## Methods of improving the representation of ozone in the Met Office Model

Camilla Mathison, David Jackson and Mike Keil

### Version History:

Version Number	Date	Approval	Summary of Changes
1.0	25-03-2007	Andrew Lorenc	First Issue version 1.0

## Abstract

Ozone is an important trace element in the atmosphere, both at the surface where it poses risks to health and in the stratosphere where it protects the earth surface from harmful ultraviolet (UV) radiation.

Ozone can potentially have a large impact on NWP products. Improved representations of ozone can lead to better temperature analyses and forecasts (via more accurate radiative heating rates) and better assimilation of satellite radiances. Improved ozone analyses can also lead to improved surface UV forecasts, and potentially the correlations between ozone and wind can be used to improve upper troposphere / lower stratosphere wind forecasts. Until recently, the availability and quality of ozone observations, and the understanding of the performance of the ozone assimilation scheme, have not been sufficient for these advances to have been realised. However, with the introduction of additional ozone observations from satellites and the growing maturity of ozone assimilation techniques it is now appropriate to revisit these issues.

The specific focus of the work presented here is to investigate whether different representations of ozone can improve temperature (and other dynamical) analyses and forecasts via changes to the radiative heating. In this report the current approach, where ozone is represented by climatology (Li and Shine, 1995), is compared with 4 other methods of representing ozone. These include

- An alternative climatology provided by the 'Stratospheric Processes And their Role in Climate' (SPARC) project.
- Use of the European Centre for Medium-range Weather Forecasting (ECMWF) ozone field in the UM.
- A 3D-Var assimilation system using two observation sources of ozone (one an operational source with observations available in real-time, the other a research instrument).
- A 3D-Var assimilation system using ozone observations from the observation source available in real-time.

The experiments were run for a 45-day period from 1<sup>st</sup> January 2006 to 15<sup>th</sup> February 2006. This period is of particular interest, because record low ozone was recorded over the UK at this time (Keil et al., 2007).

The NWP index shows a positive impact when the ozone climatology is changed from Li and Shine (1995) to SPARC. This is mainly due to the improvement in the tropics when compared against analysis. The inclusion of ozone in the assimilation system also shows improvements in comparison against analysis and observations. However, the use of the ozone ECMWF field in the Unified Model caused deterioration in the NWP index and an increase in errors and therefore would not be recommended as a way of improving ozone in our model.

The results presented here suggest that to use SPARC climatology in place of Li and Shine (1995) would be a positive first step with no additional running cost to the system. The 3D-Var systems tested here showed a positive impact on the global and extended index, thus indicating that there may be greater benefit (although also a cost) from implementing an assimilation system that included ozone. This is a positive indication that the development and testing of the ozone assimilation system should be extended to a 4D-Var system with a view to operational implementation in some form in the future.

# Contents

## 1. Introduction

## 2. Experiments

- 2.1. An alternative ozone climatology
- 2.2. ECMWF ozone in the Unified Model
- 2.3. 3D-Var Systems including ozone assimilation

## 3. Analysis of the results

- 3.1. The global index
  - 3.1.1. The extended index – comparison against analysis
  - 3.1.2. The extended index – comparison against observations
  
- 3.2. Analysis of field output
  - 3.2.1. Ozone fields
  - 3.2.2. Temperature fields
  - 3.2.3. Geopotential height fields
  
- 3.3 Comparison of ozone fields with independent data
  
- 3.4 Additional verification of temperature fields
  - 3.4.1 Comparison with EOSMLS Data
  - 3.4.2 Comparison of experiments versus analysis
  - 3.4.3 Comparison of experiments versus sonde observations

## 4. Conclusions and future work

## 5. References

## 1.0 Introduction

Ozone is widely acknowledged as being one of the most important trace elements in the atmosphere. Ozone levels at the surface can seriously affect health, meanwhile; in the stratosphere its function preserves life by forming a protective layer against the Sun's rays.

Ozone is potentially also very important within Numerical Weather Prediction (NWP) models for a variety of reasons. For example, more accurate representation of ozone may lead to more accurate assimilation of satellite radiances from channels that are sensitive to ozone, and the utilisation of correlations between ozone and wind could lead to improved wind analyses in the upper troposphere / lower stratosphere. In addition, surface ultraviolet (UV) forecasts (e.g. Austin et al, 1994) can be enhanced by utilising more accurate ozone fields.

Another way that NWP can benefit is via more accurate radiative heating rates, and hence temperatures, which arise when more accurate representations of ozone are used in the forecast model radiation scheme (this is often referred to as 'ozone/radiation interaction'). This is the focus of the experiments presented here. Recent work has shown that the ozone/radiation interaction has little clear positive impact on tropospheric temperature analyses and forecasts (e.g. Morcrette, 2003). However, with the introduction of new ozone observations from satellites and the growing maturity of ozone assimilation techniques, it is likely that a greater improvement to temperature forecasts from the ozone / radiation interaction can be demonstrated now than at the time when Morcrette did his experiments. Thus it is appropriate to revisit these issues now.

There are several possibilities investigated here for improving the representation of ozone in the Unified model (UM). Currently the Met Office use the Li and Shine (1995) climatological ozone field which includes 5 years of data on a fairly coarse resolution (2.5° by 2.5°). A first consideration for improving the ozone representation in the Unified Model was therefore to examine the impact of using a different climatology that uses a longer period and a newer data set. The alternative climatology selected for this work was from the 'Stratospheric Processes And their Role in Climate' (SPARC) project. While changing the climatology may show some improvements, it is better to have a full representation of the ozone field. In contrast to the Met Office, the European Centre for Medium Range Weather Forecasts (ECMWF) already assimilate ozone and therefore produce a full ozone field 4-times daily. Another approach considered was therefore to try and import the ECMWF ozone field into the Unified Model and establish if this improved the ozone representation in the Met Office model more than simply changing the climatology.

The above two methods for improving ozone are cheaper than running the ozone assimilation within the Met Office systems, but are not able to represent any correlation between model transport and the ozone analysis. This correlation is important at many vertical levels especially in the upper troposphere and lower stratosphere, where the temperature is highly sensitive to the ozone distribution (e.g. Cariolle and Morcrette, 2006). Two further options were therefore considered in the form of two systems that assimilated ozone observations. One used only real time observations to establish the best results that the assimilation system could produce using all the observations that are currently available operationally. The second used both real time observations and observations from a research instrument (i.e. not available in real-time), to establish if more observations at a better resolution had any impact on the results.

Each of these approaches and the results from an extended trial period are presented and compared in the following sections. Section 2 gives details of each of the experiments. Section 3 summarises and compares the results from the trials. Conclusions and recommendations for future work are given in Section 4 and References are given in section 5.

## 2.0 Experiments

Four experiments were run from the 1<sup>st</sup> January 2006 to the 15<sup>th</sup> February 2006, in addition to a control run which consisted of a standard 3D-Var system with the current UM climatology (Li and Shine, 1995) (run CTRL). Briefly, the four experiments included

- An alternative climatology provided by the SPARC project (run SPARC).
- Use of an ECMWF ozone field in the UM (run ECMWF).
- A 3D-Var system with ozone assimilated using two observation sources; one an operational source with observations available in real-time, the other a research instrument (run EOSMLS+SBUV).

- A 3D-Var system with ozone assimilated using only the observation source available in real-time (run SBUV).

In all these experiments, the forecast model used has a horizontal resolution of  $3.75^\circ$  longitude by  $2.5^\circ$  latitude and 50 vertical levels from the surface to around 0.1hPa. The model dynamical equations, including the transport scheme, have a semi-Lagrangian formulation (Davies et al, 2005), and the data assimilation uses 3D-Var (Lorenc et al, 2000). More details of each experiment are given later in this section. For the remainder of this report the experiments will be referred to using the abbreviations given in brackets.

This period in 2006 was of particular interest as it includes a period of considerable activity in the stratosphere. As a consequence of a stratospheric sudden warming that was in progress during January 2006, the polar vortex was shifted southwards over northwest Europe. This includes a period from 16 to 19 January where Polar Stratospheric Clouds were present in the vortex over the UK. Throughout most of January suitable conditions were present for ozone destruction by heterogeneous chemistry within the polar vortex. This event is described in detail in Keil et al (2007).

The initial mass and wind fields for the experiments were taken from the operational Met Office stratospheric analyses. The ECMWF ozone fields were retrieved from their MARS archive for the period 1<sup>st</sup> January 2006 to the 15<sup>th</sup> February 2006. During the period of the trial, on the 1<sup>st</sup> February 2006, ECMWF increased the vertical resolution of their model from 60 to 91 levels. Although this required some adjustment within the UM for the trial to continue, the ozone field could still be used in the UM in the same way as before.

## 2.1 An alternative ozone climatology in the UM

The first option investigated for improving ozone in the UM was to establish what improvement could be made, if any, by using an alternative ozone climatology to that currently used. It is possible that simply changing the climatology could improve the model performance sufficiently to make the assimilation of ozone, which is more expensive computationally, unnecessary. In order to test this theory the same experiment was run using SPARC climatology in the UM in place of the usual Li and Shine (1995) climatology for ozone. Figure 1 shows the zonal mean average for January 2006 of the SPARC (plot a) and Li and Shine Climatology (1995) (plot b). There are some significant differences between the two; in particular the peak of the ozone field and the tropopause height are at slightly different vertical levels.

The ozone climatology currently used in the UM is a 4-dimensional distribution of atmospheric ozone that has been built up from the combination of several observational data sets (Li and Shine, 1995). The climatology is based mainly on satellite data from the Solar Backscatter Ultraviolet radiometer (SBUV) and the Stratospheric Aerosol and Gas Experiment II (SAGE II) with supporting data from ozonesondes and other satellite instruments, such as the Solar Mesosphere Explorer (SME) and the Total Ozone Mapping Spectrometer (TOMS). Li and Shine (1995) is a global ozone climatology with a horizontal resolution of  $2.5$  by  $2.5$  degrees and 47 irregularly spaced vertical levels between 1000 and 0.0011hPa. The climatology was calculated using 5 years of data from 1985 to 1989, with one 3-dimensional data set per month. The Li and Shine climatology (1995) is generally a good representation of ozone except near the equator, where the low vertical resolution of the SBUV dataset smoothes out the ozone maximum near the tropopause. Therefore the SAGE II ozone maximum is not fully reflected in the climatology.

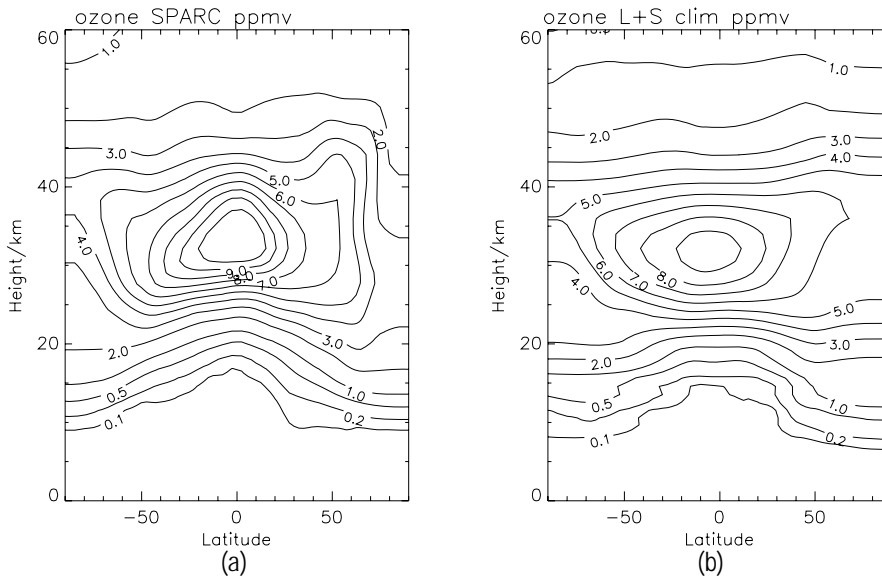


Figure 1 Plots of the two ozone climatologies considered in the experiments. Plot a shows the SPARC climatology and plot b is the Li and Shine climatology (1995). These plots are the zonal mean averages for January 2006.

The SPARC climatology is a consolidation of existing information merging model data with SAGE and TOMS ozone trends. SPARC climatology includes a global stratospheric trend dataset from the 'SPARC Ozone Trends Assessment' (Randel and Wu, 1999), which provides monthly ozone profile trend estimates above the tropopause for the period 1979-1997. Outside the polar-regions and above 20km, SAGE I/II profile trends are used and between the tropopause and 20km a combination of TOMS and SAGE column ozone trends are used. In the polar-regions ozonesonde data has been used up to a height of 27km. Kiehl et al (1999) have combined the results from an atmospheric chemical transport model with the satellite and ozonesonde data to produce a hybrid monthly ozone data set covering the period 1870 to 1990 for the troposphere and stratosphere. Hence the chemical transport model provides the information on ozone distribution in the troposphere while the stratosphere ozone trends follow those described by Randel and Wu (1999). The original data has a resolution of  $10^{\circ} \times 5^{\circ}$  with a 2km resolution in the vertical with the top level at 60 km (Karoly, 2000).

## 2.2 ECMWF Ozone in the UM

The second option investigated was the use of the ECMWF ozone field in the UM. This option was investigated as an alternative to using climatological ozone which cannot provide a full representation of ozone in the model (Section 2.1).

ECMWF currently assimilate ozone within their model using SBUV data, Global Ozone Monitoring Experiment (GOME) total column ozone and two ozone layers from NOAA-16 (ECMWF website). Figure 2 shows an example of an ECMWF ozone field in UM format, this plot shows the zonal mean average for January. A 3-dimensional ozone field is therefore available 4-times daily for retrieval from the ECMWF operational model output. This field, with some manipulation, can be used within the UM to provide a full and timely ozone field without performing the assimilation of ozone in the Met Office system.

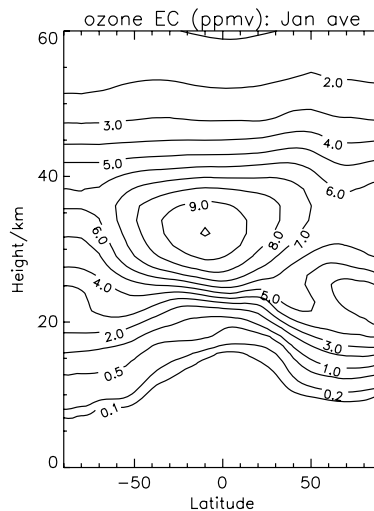


Figure 2 Zonal mean for January 2006 for ECMWF field imported into the UM.

Importing ECMWF ozone into the UM appears to be, computationally, a cheaper alternative to assimilating ozone within the Met Office 3D or 4D-Var systems; however the implementation of a field from a different model does require some extra steps in the forecast process. The ECMWF fields are output in Gridded Binary (GRIB) format at a different horizontal and vertical resolution to the Unified Model. Therefore to generate a field that the UM can use, the ECMWF ozone must be configured to the same format and vertical and horizontal resolution as the UM using the UM reconfiguration utility for converting from GRIB. The reconfigured ECMWF ozone field must then be added to the analysis using another UM reconfiguration utility to replace the 2-dimensional climatological field with the full 3-dimensional ECMWF ozone; this must occur before the model begins the forecast run. During the trial, the ozone data was retrieved from MARS for the entire period. There were some problems encountered at the beginning of February 2006 when the ECMWF model was upgraded to 91 levels. This was in the middle of the trial period and therefore required modifications to be made to the retrieval of the data and the reconfiguration from GRIB to UM format.

The extra time needed for the two reconfiguration steps, together with the requirement for the data in sufficient time prior to the forecast run for these pre-processing steps are difficult to quantify from the trials described here. These factors would need to be considered before this option could be considered for operational use.

### 2.3 3D-Var system including ozone assimilation

The third and fourth options investigated involved the development of the Met Office 3D-Var system to include the assimilation of ozone. These experiments are the more expensive of those presented here: for example, ozone assimilation could add around 10% to forecast model computation costs and up to 20-25% to assimilation computational costs. However, the assimilation of ozone has several potential benefits that could easily offset the added cost. Ozone assimilation could improve other fields e.g. temperature and wind in the following ways;

- The more accurate assimilation of satellite radiances from channels sensitive to ozone.
- Utilisation of correlations between ozone and wind to improve wind analyses in the upper troposphere and lower stratosphere (although this is not investigated here).
- Improved ozone/radiation interaction due to increased accuracy in radiative heating rates, therefore temperatures arising from the scheme (Jackson, 2004).

Two experiments were run. The first experiment demonstrates the best possible ozone assimilation that can currently be produced using the Met Office system. In this experiment the 3D-Var system is used to assimilate the usual operational dynamical observations together with version 1.51 Earth Observing System Microwave Limb Sounder (EOSMLS) ozone profiles and SBUV ozone densities. This system is described in the paper by Jackson 'Assimilation of EOSMLS ozone observations in the Met Office Data Assimilation System'. The second experiment represents the best possible ozone assimilation that can currently be produced operationally using SBUV observations that are currently the only observations available in real-time.

SBUV is an operational nadir-viewing instrument that infers the ozone vertical profile by measuring sunlight scattered from the atmosphere in the middle ultraviolet. The retrievals are provided in 12 layers but are combined at ECMWF into 6 layers in order to reduce observation correlations. The 6 layers are 0.1-1hPa, 1-2hPa, 2-4hPa, 4-8hPa, 8-16hPa and 16hPa-surface. The horizontal resolution is approximately 200km. The SBUV data was quality controlled using the same system as ECMWF; no observation with a solar zenith angle greater than 84° or a quality flag greater than zero is used (Jackson, 2004).

EOSMLS is a research instrument that uses microwave emission to measure temperature and constituents in the stratosphere and upper troposphere. Ozone mixing ratio is measured between 8 and 50km with a vertical resolution of 3km and horizontal resolution of 165km (along the suborbital track). A stratospheric ozone map is available daily, and a tropospheric ozone map is available on a monthly basis (EOSMLS webpage).

In runs EOSMLS+SBUV and SBUV, ozone is assimilated into the 3D-Var system univariately. In addition, ozone-radiation interaction is included in these experiments. In other words, the assimilated ozone fields are used in the calculation of the model radiative heating rates. It is important to note that this is different to most other Met Office assimilation experiments reported previously (e.g. Jackson and Saunders, 2002; Jackson, 2004; Geer et al, 2006ab, 2007), where the assimilated ozone is completely independent of the radiation scheme. The ozone assimilation scheme used is described in Jackson (2007) and Geer et al (2006b). The gas-phase production and loss of ozone in the stratosphere is described by the chemistry parameterisation developed by Cariolle and Deque (1986). The background error covariances used are uniform for all latitudes and longitudes and they are based on the vertical covariance data supplied by ECMWF.

### 3.0 Analysis of the Results

The analysis of the experiments outlined in Section 2 involved the use of the global index (Section 3.1) to give a broad indication of the performance for each experiment. The global index is a tropospheric based system compiled from the following parameters; mean sea level pressure, 500hPa geopotential height and the winds at 250 and 850hPa. These parameters are verified over the Tropics and both hemispheres for the forecast ranges T+24, 48, 72, 96 to T+120. Each forecast is compared with a forecast of persistence using the normalised root mean square errors to calculate a skill score. A persistence forecast is one in which the fields remain the same as the initial conditions throughout the forecast period. Further details regarding the global index are available on request.

An extended global index (Section 3.1.1) was also used to provide more detail regarding errors in individual fields; this is a more comprehensive system which incorporates stratospheric levels and more fields than the standard global index. In the extended index in addition to the fields in the global index geopotential height, winds and temperature are all verified at levels of 850, 700, 500, 250, 100 and 50hPa. Relative humidity fields are also included at 850 and 700hPa. The extended global index will simply be referred to as the extended index for the remainder of this document.

Further comparisons were made using plots of ozone, temperature and geopotential height fields from each of the experiments (Section 3.2) to investigate the results observed in the indices. Consideration of the errors in the ozone fields by comparing them with independent data is included in Section 3.3 and the additional verification of temperature fields concludes the analysis in Section 3.4.

#### 3.1 The global index

The results of the experiments described in Section 2 were compared with the control experiment, which uses Li and Shine (1995) climatology, firstly using the global index.

Table 1 shows a summary of the difference between the global index for each of the different experiments and the control run compared with both the analysis and observations. Although the global index should not be used exclusively to accept or reject a given method, it does give an initial indication of the impact of each method on the UM. It is evident from Table 1 that the relatively simple step of using a different climatology has a significant favourable impact when compared with analysis however; this is diminished when compared against observations. One possible explanation for the improvement in the comparison against analysis could be the improved representation of SPARC climatology in the Tropics compared to the Li and Shine (1995) climatology. The analysis of the Root Mean Square Errors and Mean Errors

described later in Section 3.3 support this theory. In the comparison against observations the SPARC climatology may appear to perform less well due to the scarcity of observations in the Tropics.

The use of ECMWF ozone fields in the UM has a negative impact on the global index when compared with either analysis or observations. It is entirely possible that this detriment is not a reflection on the ECMWF ozone field itself but on the fact that the field is not consistent with the UM, for example the tropopause height in the ECMWF model is known to be different to that of the UM, this would be a likely cause of degradation in the forecast. However, Figure 11 shows that in the northern hemisphere lower stratosphere the ECMWF ozone field is more inaccurate than all other ozone fields used and this may feed through to a degradation in the NWP Index. This is discussed further in Section 3.3.

In both experiments where the Met Office 3D-Var system was extended to include the assimilation of ozone, a positive impact on the global index was observed when compared against either the analysis or the observations. The improvement observed in the two assimilation systems when compared with observations was curious because run SBUV scored higher than run EOSMLS+SBUV. This could be due to a slight problem with EOSMLS data that occurred at the start of the trial period. This problem is discussed further in Section 3.2.1, where it is evident in the ozone fields, and also in Section 3.3 where it can be seen in the temperature fields. The EOSMLS instrument is a research instrument and therefore a key problem is that its data is not available in real-time. This makes it unsuitable for use as an input to an operational data assimilation system although there are other instruments on board operational satellites which will provide similar data in the near future e.g. the Global Ozone Monitoring Experiment II (GOME II); this instrument flies on board Metop from which ozone retrievals will be available in the second half of 2007. While this experiment cannot indicate exactly the impact of adding a particular set of observations not yet available, it does allow the impact of including more ozone observations to be assessed in a more general sense.

run	SPARC	ECMWF	EOSMLS+SBUV	SBUV
Global index (compared with analysis)	+0.314	-0.027	+0.413	0.112
Global index (compared with observations)	+0.051	-0.216	+0.182	+0.289

*Table 1 summary of the change to the global index using each of the experiments described in Section 2.0.*

### 3.1.1 The extended index - comparison against analysis

The extended index gives more detail than the global index discussed above, identifying which fields in each hemisphere and the Tropics compared better or worse against the control. Figure 3 summarises the forecast RMS differences for several different forecast lengths between each experiment and the control for the Northern hemisphere, the Southern hemisphere and the Tropics compared with the analysis.

Figure 3 illustrates that in both of the experiments where ozone data was assimilated (the yellow and aqua bars respectively); consistent reductions in errors were observed in most fields across the three areas. There were some fields where the errors did increase e.g. the geopotential height at 100 and 50hPa; however these fields had larger errors than all the other fields in every experiment and at almost every forecast time. The best performance overall was for run EOSMLS+SBUV. This run had the largest reduction in the RMS difference between forecast and analysis in the Northern and the Southern hemisphere (-0.4 and -1.2% respectively) and the second largest improvement in the Tropics (-1.1%).

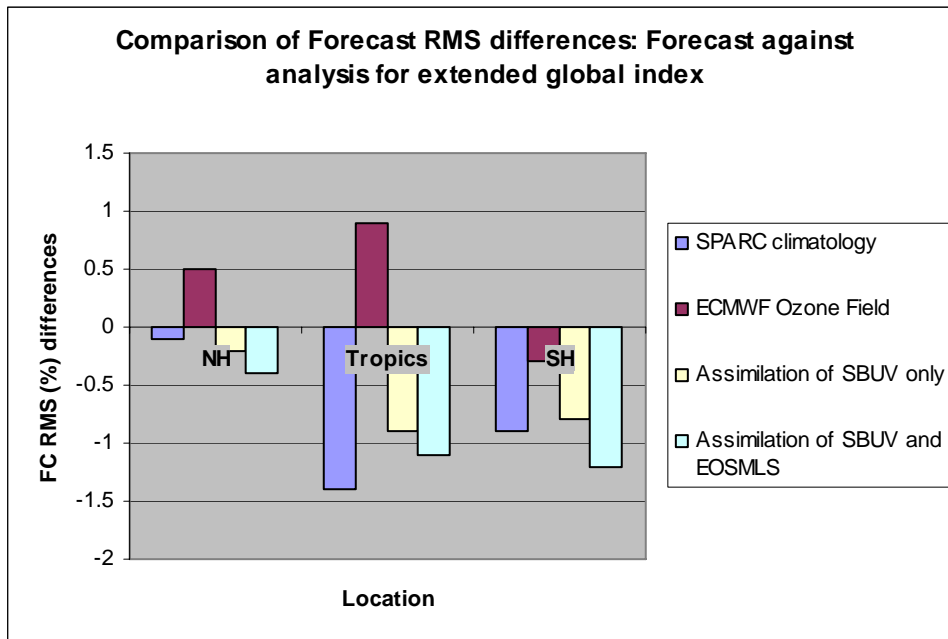


Figure 3 A comparison of forecast RMS percentage differences for a range of forecast times from T+24 to T+120 for the extended index when compared against analysis. The region of verification is given along the x axis with each coloured bar representing the difference between the experiment and the control.

Runs SBUV and SPARC performed to a similar standard in the North and Southern Hemisphere. Run SPARC showed particularly good results in the Tropics (-1.4%) and for this reason was better overall than run SBUV (which produced a score of -0.9% in the Tropics). Figure 3 clearly shows that run ECMWF was the only experiment to perform worse than run CTRL when compared against analysis in two of the three regions.

### 3.1.2 The extended index - comparison against observations

The comparison of the experiment results against observations was less positive than the comparisons against analysis, as all the methods caused an increase in the forecast RMS percentage differences (see Figure 4). The geopotential height fields at 50 and 100hPa for each of the experiments had significant errors compared with the control; the sensitivity of the extended index to these few fields could explain why all of the experiments showed an increase in errors when compared against observations. These geopotential height fields are considered further in Section 3.2.3.

Figure 4 shows the forecast RMS differences between each experiment and run CTRL for the Northern hemisphere, the Southern hemisphere and the Tropics compared with observations. As observed in Figure 3, the inclusion of ECMWF ozone in the UM causes the most significant increase in errors compared to the current Li and Shine (1995) climatology. All the percentage changes in forecast RMS differences for run ECMWF compared with observations were greater than 1.0. Figure 4 indicates that when compared with observations, the best performance overall was run SBUV. The results from this experiment revealed lower RMS errors than run SPARC in the Northern and Southern Hemispheres (yellow and purple bars respectively) and an equivalent score to run SPARC for the Tropics of 0.2%. Run EOSMLS+SBUV was better than run SPARC in both hemispheres; however, in the tropics run EOSMLS+SBUV showed an increase in RMS errors of 0.5% compared to 0.2% in run SPARC.

A better result may have been expected for run EOSMLS+SBUV when compared against observations especially in the Southern hemisphere. It is possible that this increase in errors was made worse by the problems with the EOSMLS data observed during January in the Southern Hemisphere (Section 3.1). Despite this, run EOSMLS+SBUV still showed better results than runs SPARC and ECMWF when compared with observations.

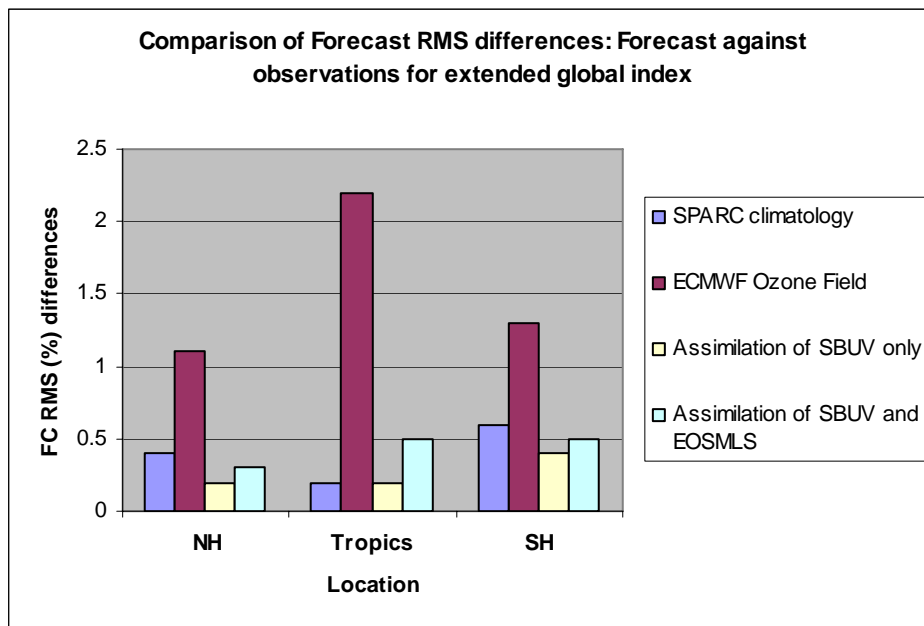


Figure 4 A comparison of forecast RMS percentage differences for a range of forecast times from T+24 to T+120 extended index when compared against observations. The region of verification is given along the x axis with each coloured bar representing the difference between the experiment and the control.

## 3.2 Analysis of field output

The NWP index and the extended index have provided useful information on the impact of each of the experiments, however in order to establish where these differences in the index come from, it is necessary to consider the fields from the experiments as well as the statistics. In this section the ozone, temperature and geopotential height fields are considered.

### 3.2.1 Ozone fields

The ozone fields were analysed, firstly to check that the ozone distribution remained realistic in each experiment and also to make any connections with the temperature fields. January (averaged for 30 days) and February (averaged for 15 days) were plotted separately, partly because of the changes made at ECMWF in the middle of the trial. The increase from 60 to 91 levels changed not only the resolution of the fields being reconfigured but also forced a change in the method used to interpolate the vertical levels from 91 to 50 levels.

Figure 5 shows the ozone zonal mean averaged for the whole of January, the problem with EOSMLS data (referred to in Section 3.1) in the Southern hemisphere is clearly visible as the dark spot in the bottom left of the plot (it is also visible in Figure 6 plot c). This error was caused by the interaction of ozone with the radiation scheme. Due to the absence of ozone observations in the troposphere, sometimes the analysed tropospheric ozone is negative, which is a consequence of how the background error covariances spread analysis increments from the stratosphere to the troposphere. In these cases, the negative ozone has to be replaced by a positive value, otherwise this will cause the radiation scheme to fail. In previous trials, a value of 0.017ppmv was used to approximate tropospheric ozone but, since this value is sometimes very different to the ozone values at neighbouring grid points, this caused the 12Z forecast to fail between 3 and 4 days into the forecast. In run EOSMLS+SBUV this was changed so that the negative ozone was replaced by a average of neighbouring, non-negative, ozone rather than by the generic 0.017ppmv value. Unfortunately, this was originally coded incorrectly and so over the first two weeks of the trial the values of ozone were too high and therefore caused this blip in the field seen in the January average. This problem was found and removed for the remainder of the trial. The problem did not occur at all in run SBUV because this was run later after the problem had been fixed. This could have caused a small adverse effect on the NWP Index for run EOSMLS+SBUV, and could explain why the NWP Index (compared to observations) was smaller than the corresponding Index for run SBUV.

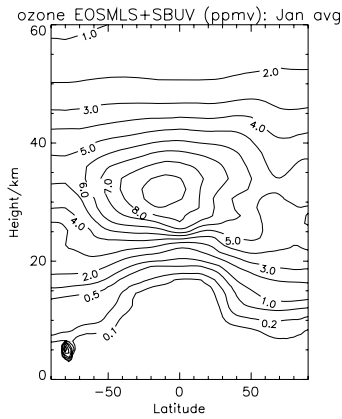


Figure 5 Zonal average for January at analysis time for run EOSMLS+SBUV.

Figure 6 shows the average differences at analysis time for January between the experiment ozone fields and run CTRL. All 4 plots show a reduction in the ozone concentrations at about 20km, i.e. in the lower stratosphere, compared to Li and Shine climatology (1995). Run SBUV shows the most widespread reduction (dotted lines) in tropospheric ozone while run ECMWF shows the most widespread increase in tropospheric ozone concentrations for the January and February averages. The analysis plots for February are not shown although these show a very similar picture.

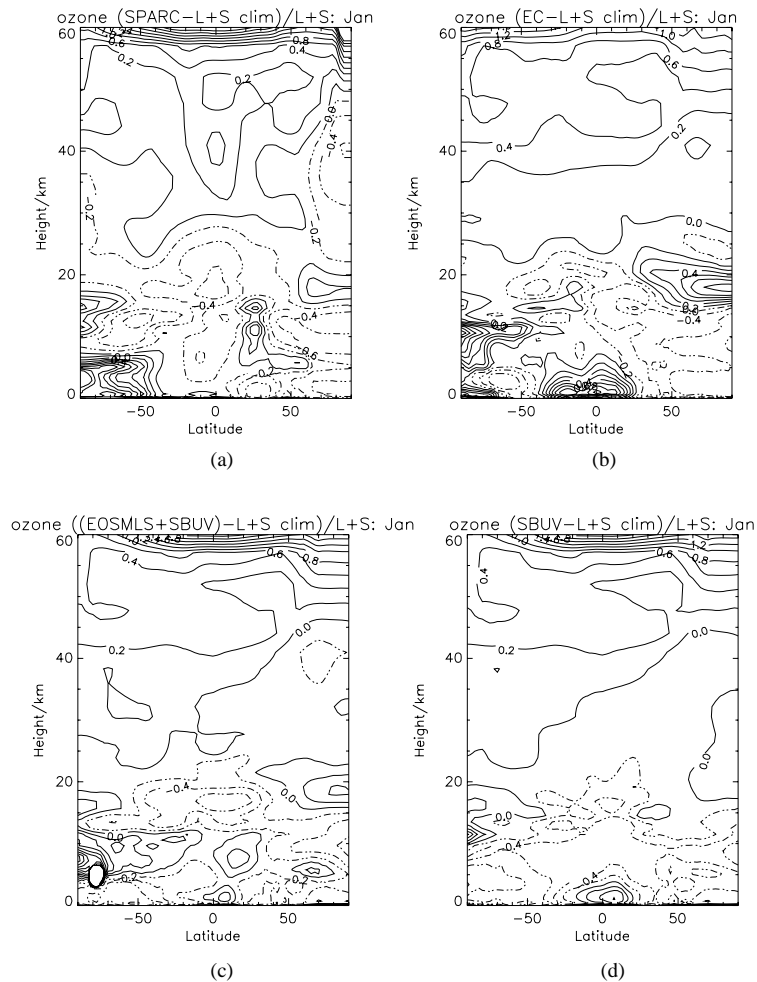


Figure 6 The difference between the experiment and run CTRL average ozone fields for January 2006. Plot a is the difference for run SPARC, plot b run ECMWF, plot c run EOSMLS+SBUV and plot d run SBUV.

Figure 7 shows three plots of the differences between ozone fields from the runs SBUV, EOSMLS+SBUV and ECMWF and run CTRL for T+24 for February. Comparing these plots to the corresponding plots for January (not shown) the differences were minimal. In general all the T+24 plots show a reduction in ozone concentration at about 20km between -50° and +50° latitude. They also show an increase in tropospheric ozone at the South pole especially in run EOSMLS+SBUV. In run ECMWF the increases in ozone observed appear to be spread over a wider area than the other runs in which ozone is assimilated; the increases in ozone in run EOSMLS+SBUV and SBUV are much more localised.

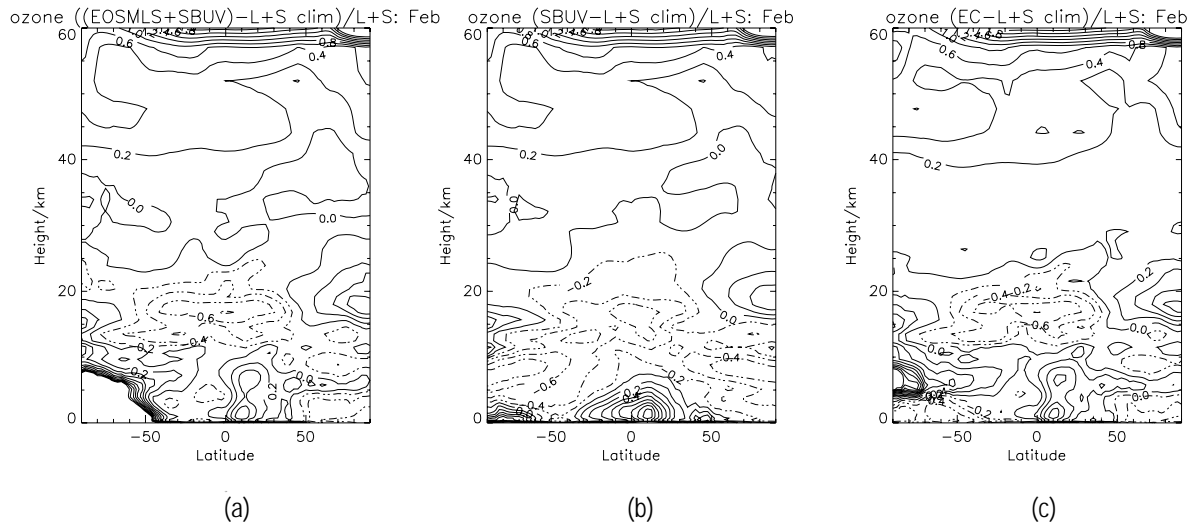


Figure 7 The difference between the experiment and run CTRL average ozone fields for T+24 of February 2006. Plot a is the difference for the run EOSMLS+SBUV and plot b run SBUV. Plot c is the difference for run ECMWF.

### 3.2.2 Temperature fields

The temperature fields were considered alongside the ozone plots. In general the differences between each experiment and run CTRL are more obvious at T+24, these fields are shown for February in Figure 8. The solid lines show the regions where there is a temperature increase and the dotted lines show the regions where there is a temperature decrease in comparison with Li and Shine (1995).

At upper levels, between 0.1 and 1.0hPa, there is an increase in temperature of the order of 10K caused by increased ozone concentration at these levels; the high incidence of solar radiation combined with the high concentration of ozone causes the largest temperature change at these levels. Immediately below this layer at approximately 1 to 5hPa, the temperatures are reduced. The increased ozone between 1.0 and 0.1hPa absorbs the radiation before it can reach the layer below and therefore acts as a barrier preventing the radiation from heating this region. In the stratosphere the changes in temperature are smaller of the order of 1K, and this reduces further in the troposphere where the changes in temperature are of order of 0.1K.

In general the sign of the ozone differences in the upper troposphere and lower stratosphere are the same as the sign of the differences in temperature at these levels; this is due to the absorption by ozone of long-wave radiation emitted from lower levels.

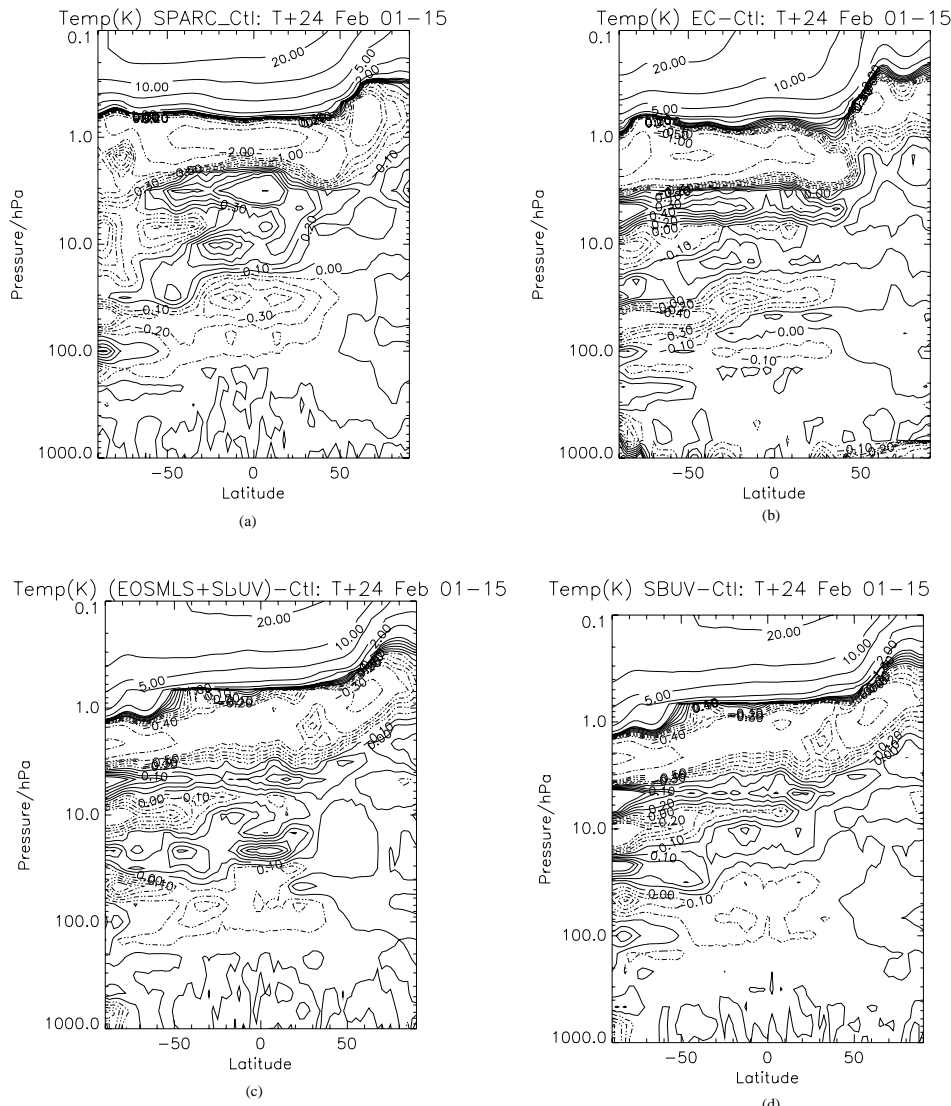


Figure 8 The difference between the experiment and run CTRL average T+24 temperature fields for the February 2006 part of the trial. Plot a is the difference for run SPARC , plot b run ECMWF, plot c run EOSMLS+SBUV and plot d run SBUV.

The radiative relaxation time in the lower to middle stratosphere is long compared to the troposphere. Haynes (2005) estimates it is 20-40 days, and Cariolle and Morcrette (2006), when running a series of experiments with different ozone climatologies, noted that temperature differences between pairs of experiments took around 60 days to establish in the lower stratosphere. Therefore, the full extent of the impact of different representations of ozone on the temperature field may not be adequately seen in the 5 day forecast period typically used in the experiments run here. Accordingly, 60 day forecasts were also run once per day for runs CTRL and EOSMLS+SBUV. The differences in February mean temperatures between these runs for various forecast lengths are shown in Figure 9. The pattern of the T+120 forecast difference is similar to the T+24 difference shown in Figure 8c, but the size of the difference is greater – for example around -0.5K near 100hPa instead of around -0.1K. By T+960 and T+1440 this difference has grown to around -2.0K. In addition, at T+480 and beyond there are noticeable differences to the temperature fields in the troposphere, whereas at T+24 and T+120 little or no differences are seen at those levels. The pattern of these differences is also fairly consistent between T+480 and T+1440. This suggests that a change in the representation of ozone may also have an important impact on the quality of extended range or even seasonal forecasts.

In the mid-stratosphere and above, the temperature differences are generally similar for all forecast lengths, which suggests that the radiative timescales are shorter there; Haynes (2005) quoted a relaxation timescale of 5 days in the upper stratosphere. An exception is the winter stratosphere, where the pattern and size of the temperature differences varies a lot. This is probably due to the large dynamical variability of the winter stratosphere.

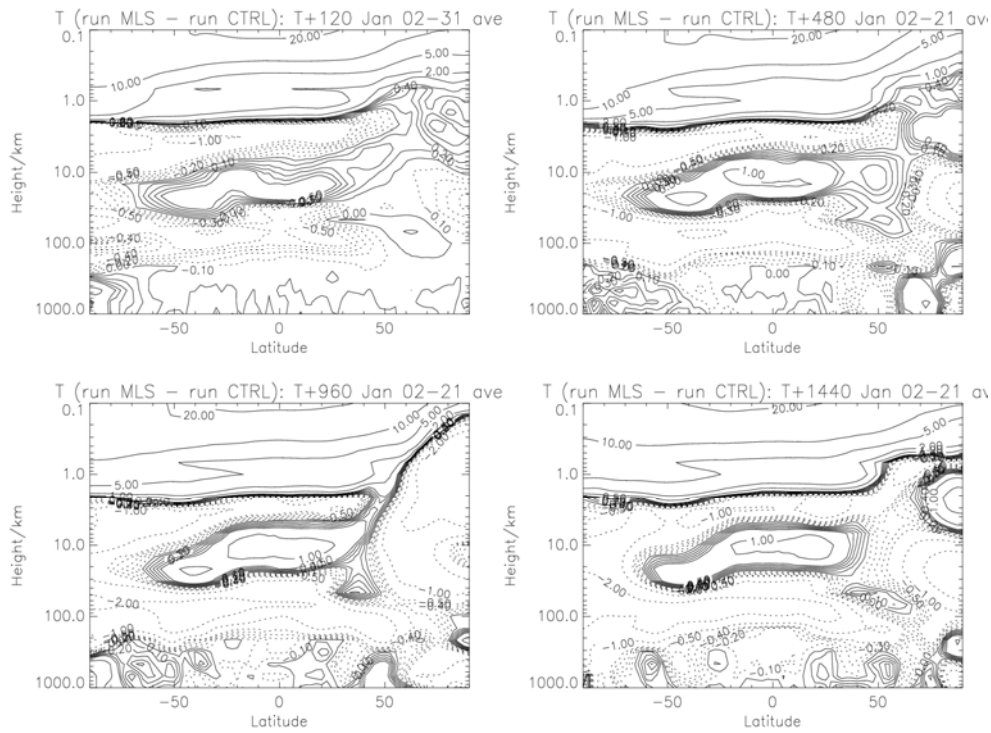


Figure 9 Like Figure 8c, except that T+120 (top left), T+480 (top right), T+960 (bottom left) and T+1440 (bottom right) temperature forecast fields for January 2006 are shown.

### 3.2.3 Geopotential height fields

The Geopotential height fields were studied to investigate the results from the extended index which indicated that there was an increase in the errors for the geopotential height fields particularly at 50 and 100hPa. It therefore seems plausible that some differences between the experiments and the Li and Shine climatology should be visible in these fields.

The geopotential height field for the Northern and Southern hemisphere were considered at 10, 50 and 100hPa. In some runs small regions of the same geopotential that were close together were merged to make bigger regions and in others they were fragmented but there were no systematic differences and no real changes in the overall large-scale structure between experiments. Figure 10 shows the geopotential height at 100hPa 24-hours into the forecast for each experiment on a single day in February; this Figure illustrates that using typical contour intervals of 200m for geopotential the typical differences between fields are small. The main region to note here is the difference in the top left section of each field (pale green). The different experiments show varying degrees of segmentation but in general the differences are quite small. This is a typical example of the differences observed in each of the geopotential height fields examined. A change of this magnitude although important in the context of the extended index is not at all obvious from examining the geopotential height maps.

## February 2006 T+24 6th February 100hPa Geopotential Height

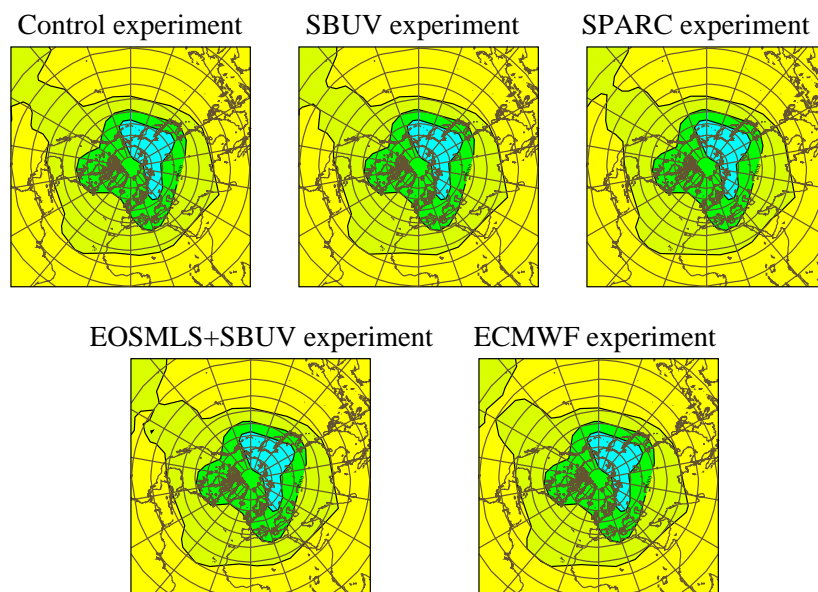


Figure 10 Geopotential height field at 100hPa for the Northern hemisphere on February 6th 2006 for all the experiments.

### 3.3 Comparison of ozone fields with independent data

Prior to investigating the impact of the different representations of ozone on temperature analysis and forecast errors, it is useful to calculate the errors in these ozone fields by comparing them with independent data.

First, these ozone fields are compared with ozone observations made by ozonesondes. Ozonesonde profiles have been obtained from the World Ozone and Ultraviolet Radiation Data Centre (WOUDC, <http://www.woudc.org/>). Most sondes are of the Electrochemical Concentration Cell (ECC) type, but some are Carbon-Iodide or Brewer-Mast sondes. The total error for the ECC sondes is estimated to be within -7% to 17% in the upper troposphere, +/- 5% in the lower stratosphere up to 10hPa and -14% to +6% at 4hPa (Komhyr et al, 1995). Errors are higher in the presence of steep ozone gradients and where ozone amounts are low. Furthermore, a laboratory comparison of the three sonde types (Smit et al, 1998) shows that the precision of the non-ECC sondes is about +/- 10-15%, compared to +/- 5% for the ECC sondes. The relative precision is best for all sondes in the middle stratosphere where ozone is a maximum. The results of short term ozonesonde intercomparison campaigns (eg Beekmann et al, 1994; Kerr et al, 1994; Smit et al, 1998) indicate that in the lower stratosphere (12-27 km) the systematic difference between sonde types is less than 5% and the random variability from one sonde to another is less than 5% for all sonde types.

Figure 11 shows the mean and standard deviation of the analysis error for the ozone used in the various experiments. A negative mean error indicates that the analysed ozone exceeds the ozonesonde observations. Therefore, in the tropics, the analysed ozone field near 100hPa is overestimated in all cases. The smallest errors are for run EOSMLS+SBUV. Jackson (2007) showed that the Met Office ozone analyses can be inaccurate in the tropical tropopause region due to errors in model transport and that the addition of EOSMLS data acts to greatly alleviate these errors. A consequence of these errors is a smearing of the strong gradient between upper tropospheric and lower stratospheric ozone and the large errors also seen in the other runs may indicate that these ozone fields also underestimate this gradient.

In the northern hemisphere the smallest mean errors are also seen in run EOSMLS+SBUV, but runs SBUV, SPARC and CTRL do a reasonable job of representing the ozone field, at least at levels above 100hPa. However, run ECMWF analyses perform poorer here, with an overestimation of 30% seen near 50hPa (See Figure 11 bottom left plot, red curve). This pattern is consistent with the higher ECMWF ozone values seen in this region in Figures 6b and 7c and could indicate that the ECMWF system is failing to represent winter polar ozone depletion adequately.

In both geographical areas, the smallest standard deviations of the analysis errors are generally seen in run EOSMLS+SBUV, and run SBUV standard deviations are also small in the northern hemisphere. This indicates that these runs tend to represent the variability of the observed ozone field better than the other runs. Not surprisingly, the standard deviations of the fit to the two climatologies, which do not represent any zonal asymmetry, are generally largest.

The differences in the mean errors shown in Figure 11 often correspond to the differences between the mean ozone fields shown in Figures 6 and 7. However, this is not always the case, since the ozonesonde observations are sparse and the temporal and spatial sampling is quite poor. An alternative way of assessing the quality of the ozone analyses is to compare them with the EOSMLS data, which have a higher horizontal resolution (around 5000 points per day) and extend up to the stratopause. The larger amounts of data means that the errors can be calculated in 5° latitude bins, instead of the 60° bins used for the ozonesonde errors, and hence one can get a better idea of the variation of error with latitude. Of course, ozone errors with respect to EOSMLS observations is not a good method of assessing the ozone analysis which includes EOSMLS data (run EOSMLS+SBUV), since the verifying data are not independent, but it is a good way of validating the other ozone analyses.

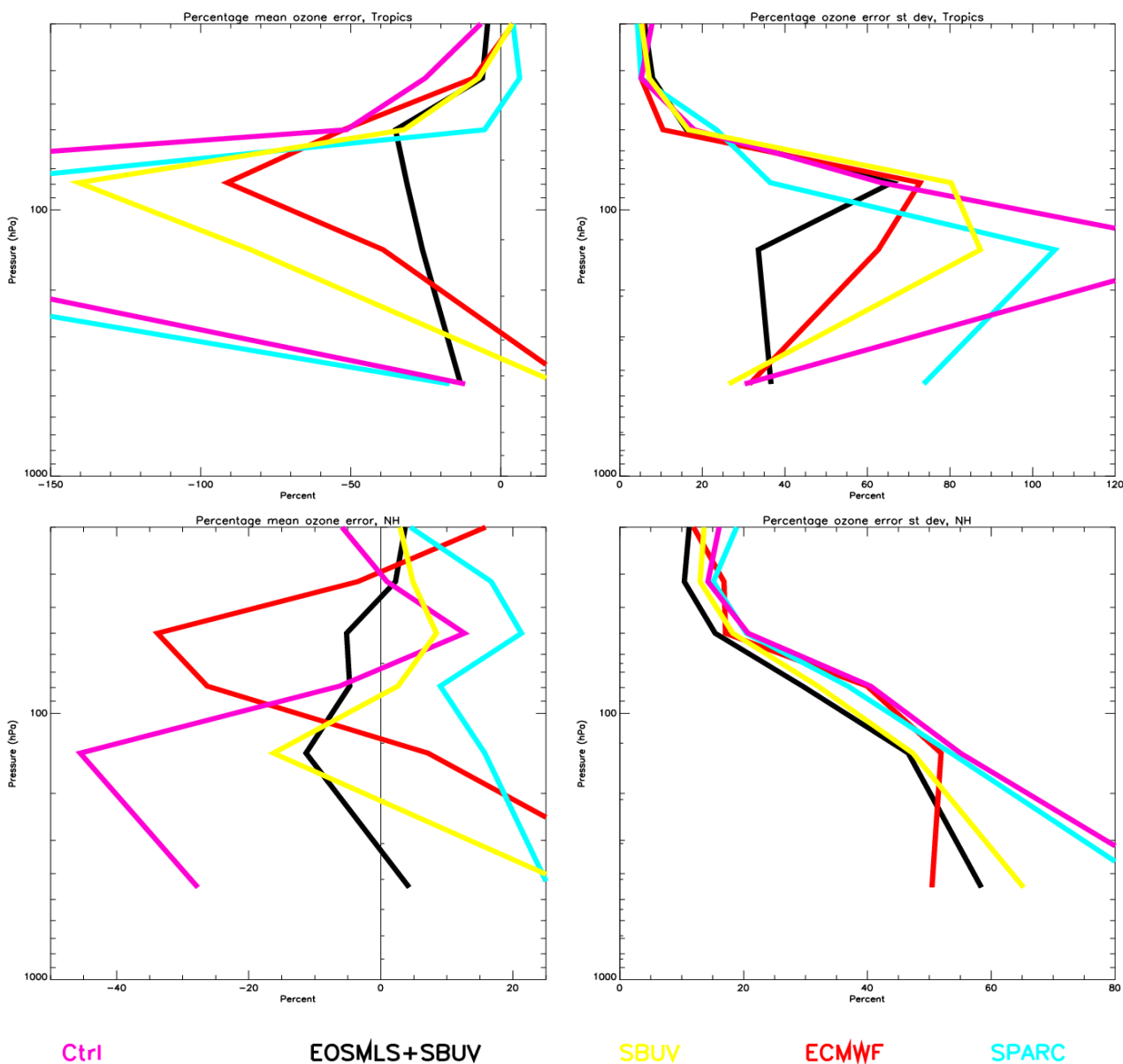


Figure 11 Mean (left panels) and standard deviation (right panels) of the ozone analysis error, calculated with respect to ozonesondes for 30°S-30°N (top) and 30°-90°N (bottom). These are normalised by the ozonesonde observations and expressed as a percentage. A positive mean error indicates that the ozonesonde ozone exceeds the analysed ozone. Black: run EOSMLS+SBUV; yellow: run SBUV; red: run ECMWF; light blue: run SPARC; purple: run CTRL.

Figure 12 shows the mean and standard deviation of the ozone analysis error, calculated with respect to EOSMLS observations for runs CTRL, SBUV, ECMWF and SPARC. As in Figure 11, a positive mean error indicates that the analysed ozone is less than the verifying ozone observations. Figure 12 confirms that the largest relative errors are near the tropopause, and the errors for run CTRL in this region are generally larger than those for the other runs, thus confirming what is shown in Figures 6 and 7. The standard deviation of the error is also generally largest for run CTRL.

Since the Li and Shine climatology was calculated in the 1990s and the other fields are derived using more recent data, it is possibly not surprising that it does not appear to represent the observed ozone field as well as the other ozone analyses.

Note also that the Li and Shine climatology (run CTRL) underestimates ozone at most levels above 10hPa. However, in runs SBUV, SPARC and ECMWF ozone is larger and the underestimate with respect to EOSMLS ozone is generally smaller. Exceptions are for run SPARC in the northern high latitudes, where ozone is even more underestimated than in run CTRL, and for run SPARC in the tropics, where ozone is overestimated by around 10-20%, instead of underestimated by 10-20%, as in run CTRL.

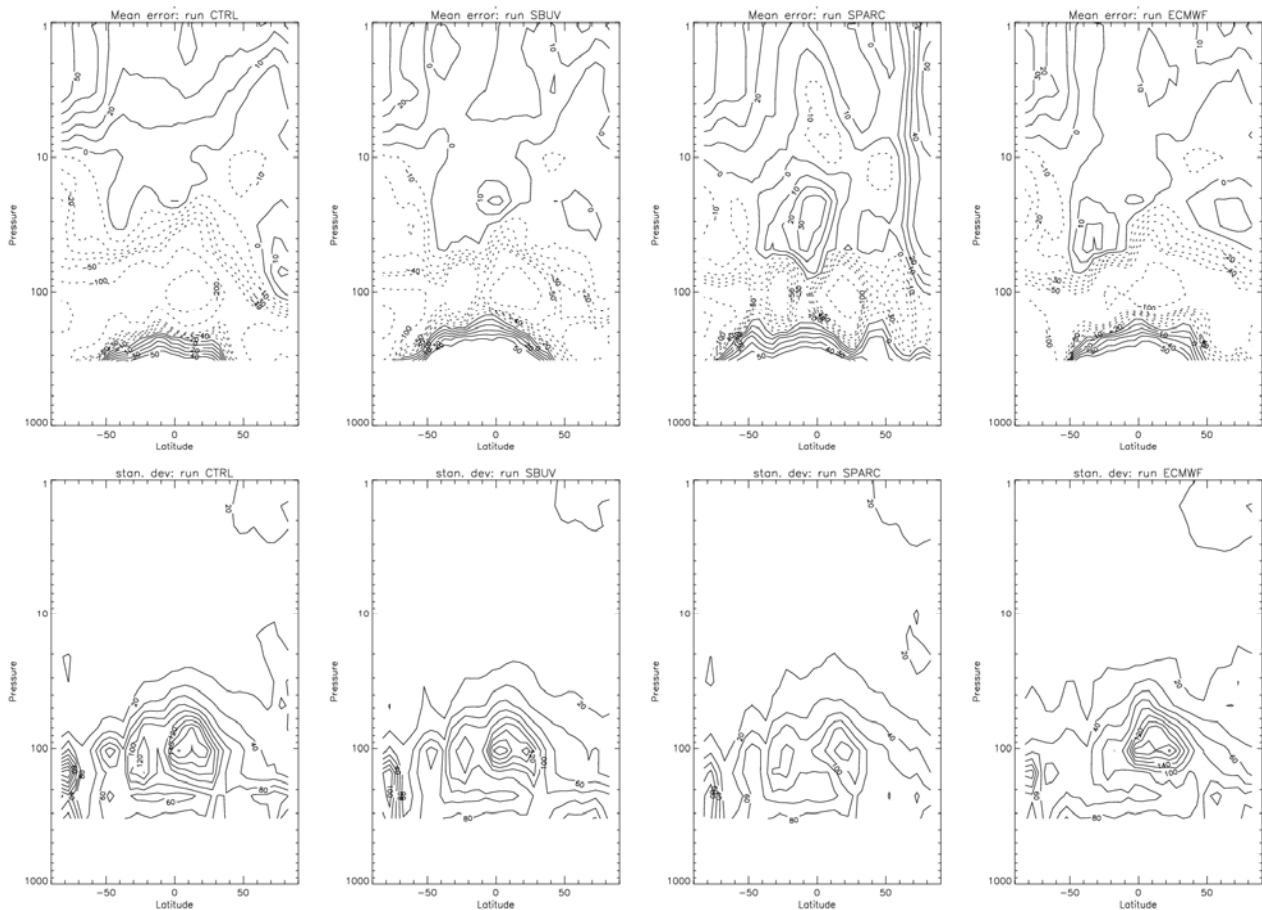


Figure 12 Mean (top panels) and standard deviation (bottom panels) of the ozone analysis error, calculated with respect to EOSMLS ozone observations in  $5^\circ$  latitude bins. Errors are shown for run CTRL (extreme left), run SBUV (left centre), run SPARC (right centre) and run ECMWF (extreme right). These are normalised by the EOSMLS observations and expressed as a percentage. A positive mean error indicates that the EOSMLS ozone observations exceed the analysed ozone.

### 3.4 Additional verification of temperature fields

The analysis so far has focused on the index scores and considered the impact on the fields for each experiment. The analysis of the forecast verification statistics for the temperature fields provides a more qualitative comparison between the experiments. In the first instance the temperature analyses in the stratosphere and lower mesosphere have been compared against EOSMLS temperature retrievals to assess the quality of the temperature analyses against observations (Section 3.4.1). The Met Office verification system (VER) output was then used to consider the troposphere and lower stratosphere by examining the errors between the forecast and analysis and between the forecast and sonde observations at different locations. The results were displayed in three different ways; a time-series illustrated the change in the RMS and mean error statistics for each experiment over the duration of the trial, a mean level plot showed their variation with pressure level and a third plot showed their mean variation with forecast time. These results appear in Sections 3.4.2 and 3.4.3.

### 3.4.1 Comparison with EOSMLS data

Here, EOSMLS temperature retrievals are used to validate the temperature analyses from the various experiments. Note that none of these data are assimilated in the experiments, and hence they are independent and suitable for verification purposes.

Initial assessment (Froidevaux et al, 2005) suggests that the EOSMLS temperatures have a warm bias of 1K in the lower to middle stratosphere, rising to around 2K in the middle and upper stratosphere. This estimate was derived from comparisons with CHAMP GPS occultation measurements, which have an advertised mean bias of less than 0.1K in the stratosphere. A later analysis (Livesey et al, 2005) reports a vertical resolution of 7-8km from 316 to 100hPa, 4km from 31.6 to 6.8hPa, 6km at 1hPa and 9km at 0.1hPa. They confirm Froidevaux's warm bias of 1-2K in the lower to middle stratosphere (100-14.7hPa). At 10hPa the bias is 2-4K, and above that level the bias oscillates in height, being warm by 1K between 6.8 and 4.6hPa, warm by 3K between 3.16 and 2.15hPa, and having zero bias between 1.47 and 1hPa.

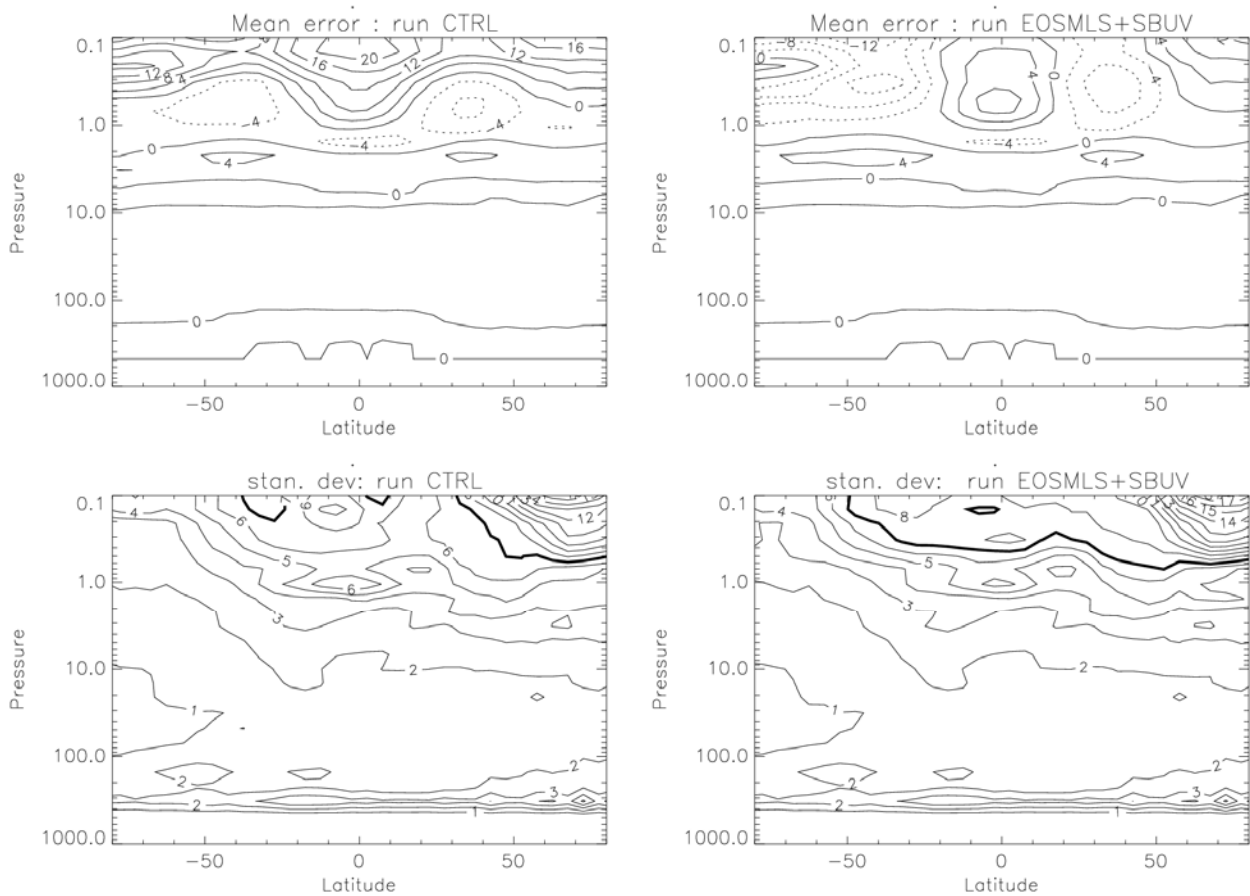


Figure 13 Mean (top panels) and standard deviation (bottom panels) of the temperature analysis error, calculated with respect to EOSMLS temperature retrievals in  $5^\circ$  latitude bins: run CTRL (left) and run EOSMLS+SBUV (right). Units: K. The 7K contour on the standard deviation plots appears in bold for clarity. A positive mean error indicates that the EOSMLS temperature retrieval exceeds the analysed temperature.

Figure 13 shows the mean and standard deviation of the temperature analysis error, calculated with respect to EOSMLS temperature retrievals. For run CTRL, there is an oscillation in bias between 10 and 1hPa which has been noted in operational stratospheric analyses and in the N320L50 parallel trail suite (PS9). Between around 1 and 0.5hPa there is a large negative bias in the analyses at the tropics and a large positive bias at other latitudes, whilst above 0.5hPa the analyses are less than the observations at all latitudes. The standard deviation of these errors increases with height, and is largest in the winter lower mesosphere. The mean errors and the standard deviation for run EOSMLS+SBUV are very similar to run CTRL below the 5hPa level, but above that level the mean errors are more positive near 2-3hPa and considerably more negative above around the 0.6hPa level. This is consistent with the temperature differences shown in Figure 8. The general impact of these changes is that above 0.6hPa the mean error for the assimilation run is similar-sized, or smaller, than for run CTRL in the tropics and high latitudes, and has switched from large and positive to large and negative at other latitudes. In addition, the fit between the run EOSMLS+SBUV temperatures and the EOSMLS

temperatures, as indicated by the standard deviation, is generally poorer than for run CTRL near and above the stratopause, except at low latitudes near 1hPa.

Corresponding mean and standard deviations for runs SBUV, SPARC and ECMWF are generally similar to those for the EOSMLS+SBUV assimilation run. This is not surprising, given the broad similarities in the ozone and temperature fields shown in Figures 6-8, and the similarity in ozone errors shown in Figure 12. These results show that although the replacement of the Li and Shine climatology with other ozone representations improves forecasts in the troposphere (as evidenced by improvements in the NWP Index); these changes can still degrade the temperature analyses at lower mesospheric levels. At such levels, solar radiative heating is highly sensitive to the ozone distribution. Recent work has indicated that the radiation scheme at these levels may be deficient and that improvements are required (Zhong and Haigh, 2001; Thelen, 2006). These upgrades should be tested alongside any upgrade to the representation of ozone within the NWP system.

### 3.4.2 Comparison of results versus analysis

The experiment results were analysed using plots of the forecast mean, mean error and RMS for four geographical regions as specified in the verification system; Australia, North America, Asia and Europe.

In general the plots showing the variation with pressure level of both the mean and RMS error are largely in agreement with each other up to approximately 1hPa at many of the different forecast times. Figure 14 shows an example for the mean (Figure 14 a) and the RMS (Figure 14 b) variation with pressure level for Europe at T+48. The pattern illustrated in Figure 14 shows that above 1hPa the mean temperatures and RMS tend to diverge slightly. This is true for all the regions for which these plots are produced and the pattern is also evident in the time-series and the plots of the temperature against forecast range at several different pressure levels.

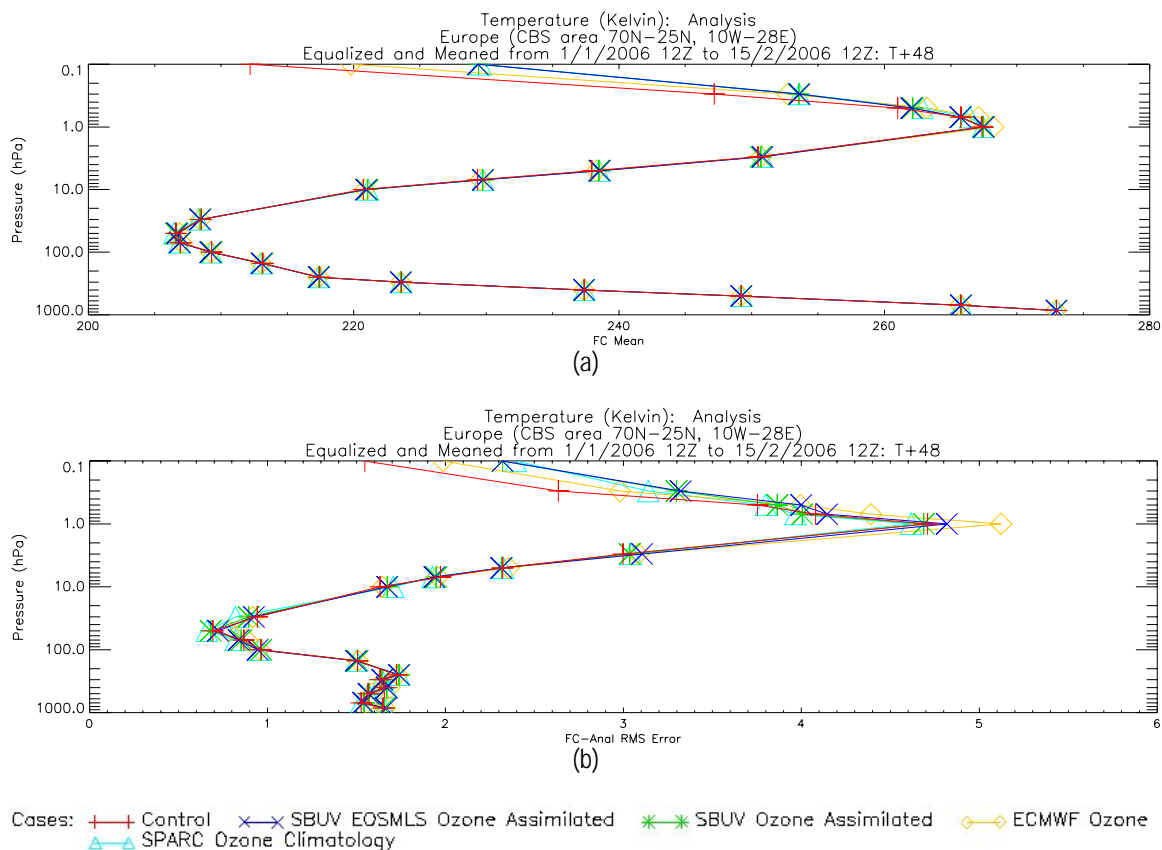
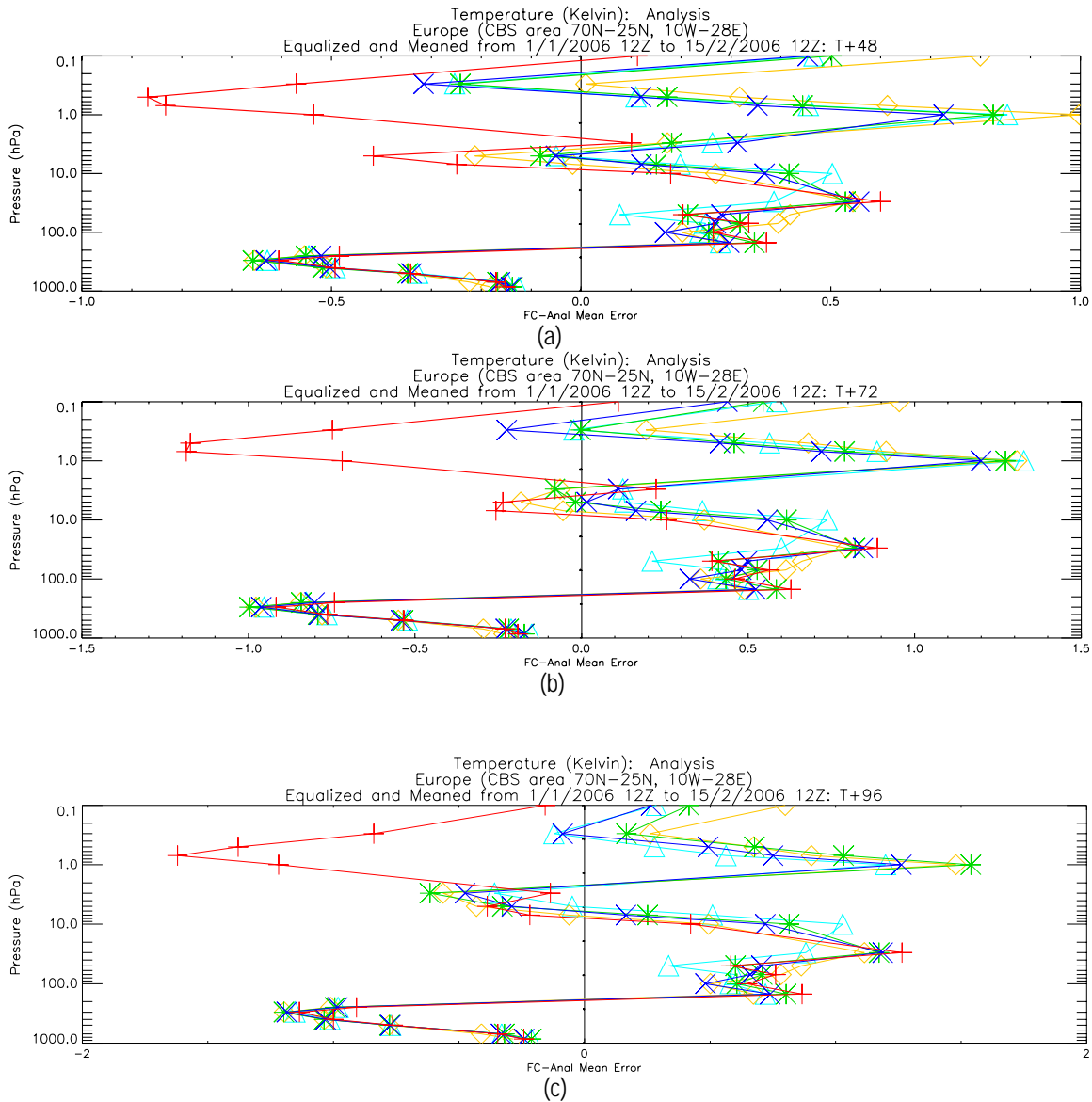


Figure 14 Variation of the T+48 temperature field over Europe with pressure level. Plot (a) shows the variation of the forecast mean temperature with pressure level. Plot (b) shows the change in forecast - analysis RMS error with pressure level.

The plots showing the change in the mean error with pressure level show more variability than those in Figure 14, although there is a lot of agreement for all of the experiments through the troposphere and the lower stratosphere. Figure 15 shows three plots of the variation of the forecast - analysis mean error with pressure level for the European region at T +48, T+72 and T+96 forecast times. Above 10hPa considerable differences develop between the mean error of run

CTRL and the other experiments. Above around 2hPa the mean error of run CTRL is considerably more negative than that for the other runs. This is also evident in the other plots of other regions.

Such differences indicate a bias between the forecast model and the analysis, suggesting either a bias in the ozone representation or in the model radiative heating due to ozone at these upper levels. Figure 12 shows that mean ozone errors with respect to EOSMLS observations are generally larger at Northern-mid latitudes in the upper stratosphere for run CTRL than for the other runs, but the absolute bias in temperature for all runs in this region is similar (Figure 15). This tends to suggest that there is a problem with the representation of radiative heating due to ozone in the model that needs to be addressed.



Cases: + Control x SBUV EOSMLS Ozone Assimilated \* SBUV Ozone Assimilated ◇ ECMWF Ozone △ SPARC Ozone Climatology

Figure 15 Variation of the forecast -analysis mean error with pressure level. This example is for Europe. Plot a is for T+48, b is for T+72 and c is for T+96.

The time-series plots in Figure 16 are for the North America region at 850hPa for the forecast time of T+24 (Plot a) and 50hPa for the forecast time of T+48 (Plot b). Plot (a) and (b) show the variation of the mean forecast error for the duration of the trial with pressure level. Both plots shown in Figure 16 are examples for a particular region, in this case North America, of a forecast time and pressure level when run ECMWF (yellow diamonds) has a larger mean error than the other experiments particularly for January. In February the mean errors for run CTRL, SPARC, SBUV and EOSMLS+SBUV increase to be similar to those for run ECMWF. This pattern is also true at other pressure levels and for other regions. In general ECMWF has the largest mean errors of all the experiments and is clearly the outlier. This may indicate that a problem arises from the imported ECMWF ozone analyses being inconsistent with the forecast model

transport, and thus the ozone field implied by that transport. The runs CTRL and SPARC may also have such an issue, however, in those cases it is likely to be less severe since these fields use ozone climatologies that are slowly varying from day to day; therefore reducing the scope for inconsistencies between the climatologies and the model transport.

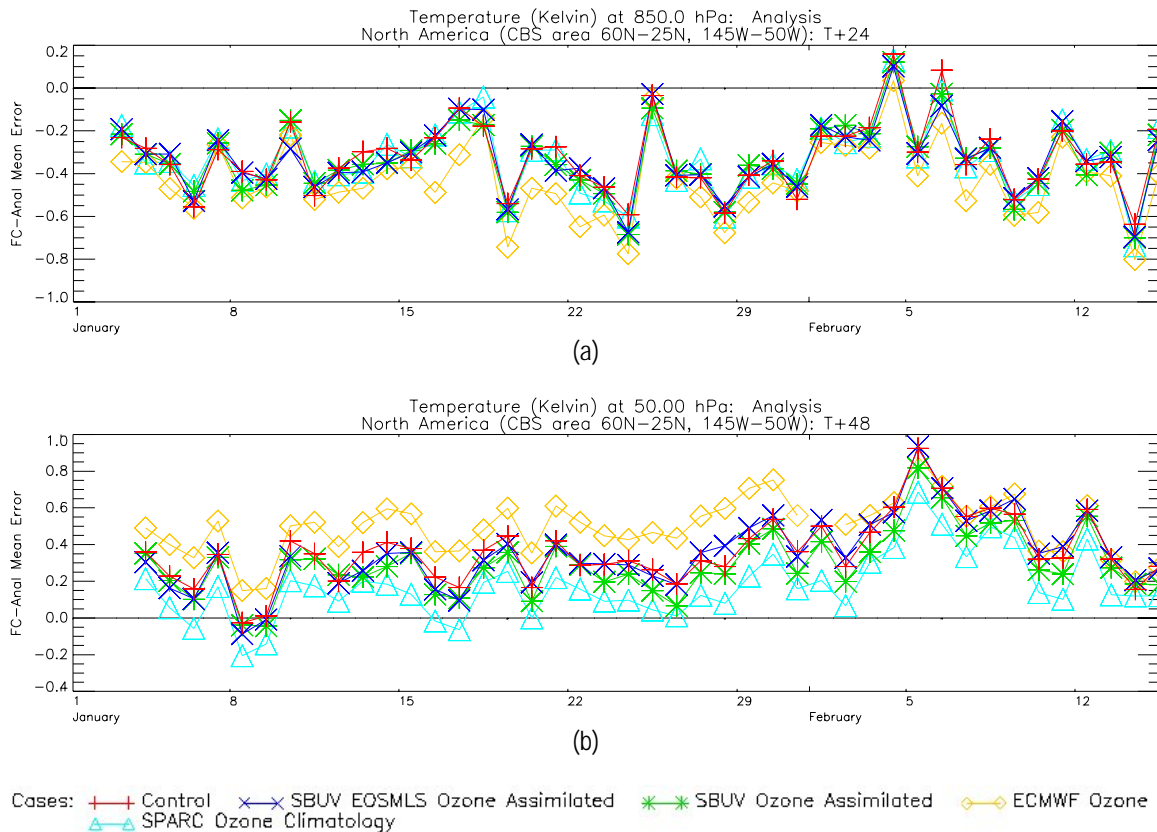


Figure 16 Time series of the forecast - analysis mean error for North America. Plot (a) shows T+24at 850hPa and plot (b) shows T+48at 50hPa

At 50hPa (and 30hPa, although this pressure level is not shown) run SPARC had the smallest mean errors (See Figure 16 plot (b), pale blue diamonds) closely followed by runs EOSMLS+SBUV and SBUV. If we consider the performance of each system for each of the four geographical regions of the globe, it appears that the runs that use ozone climatologies (runs SPARC and CTRL) have small mean errors for North America and Asia compared with the other experiments. The data assimilation experiments are generally good across all areas but are the best for Europe. In Australia run SPARC does well to reduce the mean errors but not the RMS errors. The RMS errors are very similar for all the experiments and show only small variability across the four regions.

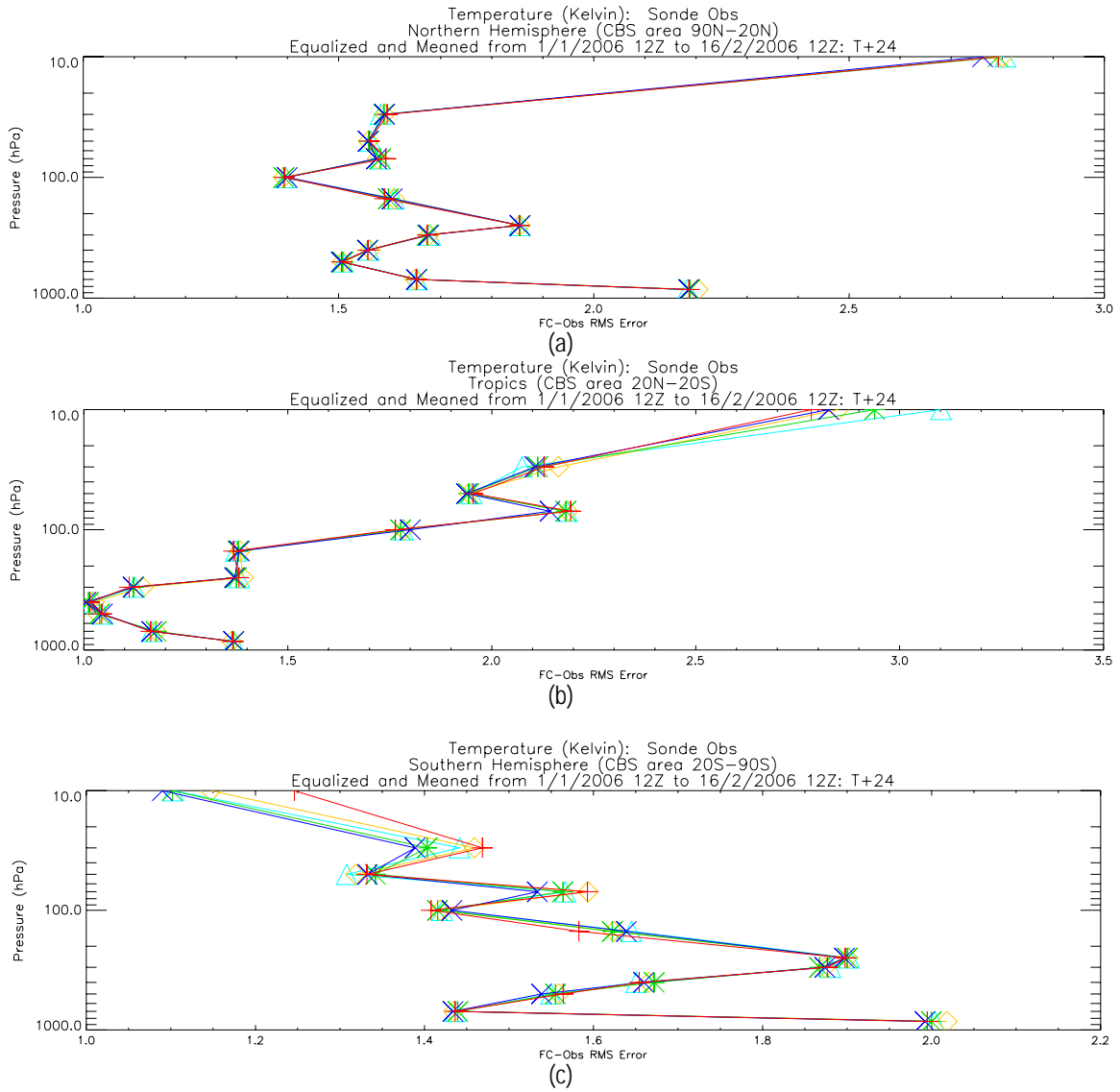
### 3.4.3 Comparison of results versus sonde observations

The experiment results were compared against sonde observations using the mean error and RMS error of the difference between the forecast and sonde observations. The plots generated in this comparison were for the larger areas of the Northern and Southern hemispheres and the Tropics. These areas are larger than in the comparison against analysis due to the sparsity of sonde observations. In order to gain a meaningful signal the smaller regions are grouped together.

Figure 17 shows the T+24 plots of the variation of forecast – sonde RMS errors with pressure level for each of the Northern hemisphere (plot a), the tropics (plot b) and the Southern hemisphere (plot c). These plots illustrate how small the differences are in the RMS errors between the different geographical areas at T+24. There was more variability in the Southern hemisphere and Tropics RMS errors than those in the Northern hemisphere; the Northern hemisphere RMS error remained very similar for all experiments at all forecast lengths.

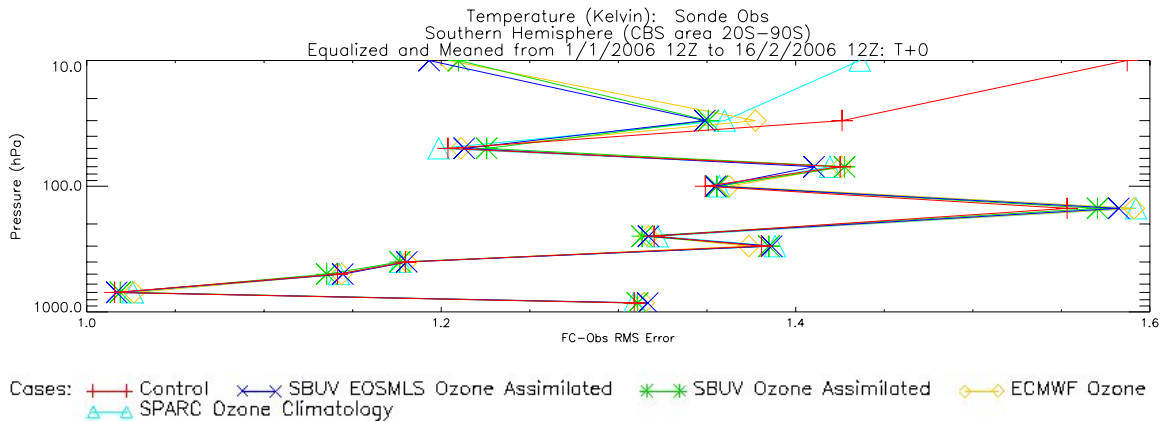
In the Southern hemisphere the differences in RMS errors were more apparent at T+0. Figure 18 shows that runs CTRL and ECMWF had significantly larger RMS errors than the other three experiments, but that by T+24 (Figure 17(c)) these errors had reduced to the equivalent of the other experiments. It appears that the use of a complete ozone field, either

an imported ozone field or assimilated one, is improving the representation of the temperature field at upper levels and thus reducing the RMS errors at analysis time.



Cases: + Control x SBUV EOSMLS Ozone Assimilated \* SBUV Ozone Assimilated ◊ ECMWF Ozone  
 △ SPARC Ozone Climatology

Figure 17 Plots comparing the variation of the RMS error with pressure level. Plot (a) is the Northern hemisphere, (b) is the Tropics and (c) the Southern hemisphere for T+24.



Cases: + Control x SBUV EOSMLS Ozone Assimilated \* SBUV Ozone Assimilated ◊ ECMWF Ozone  
 △ SPARC Ozone Climatology

Figure 18 Variation of the forecast - observations RMS errors with pressure level in the Southern hemisphere at T+0

Figure 19 shows the mean forecast errors at different forecast lengths and illustrates that there is a large spread between experiments in the upper troposphere and lower stratosphere. Most variability between experiments is again observed in the Southern hemisphere and the tropics; this is supported by the plots in Figure 17. The spread in mean errors shown in Figure 19 gradually increases as the forecast progresses but in all cases the temperature increases towards the end of the forecast; this appears to be the model attempting to reduce the cold bias that is evident in all the experiments. Figure 19 also shows that the relative order of the errors for each run does not change with forecast length (i.e. run CTRL errors are always more positive and run EOSMLS+SBUV the most negative) and this confirms what is shown in Figures 8 and 9 regarding the pattern of zonal mean temperature differences with increasing forecast length.

The warming tendency shown in Figure 19 is consistent between 150 and 10hPa but between 850hPa and 250hPa there is a downward trend in the biases indicating cooling in the troposphere at all forecast lengths.

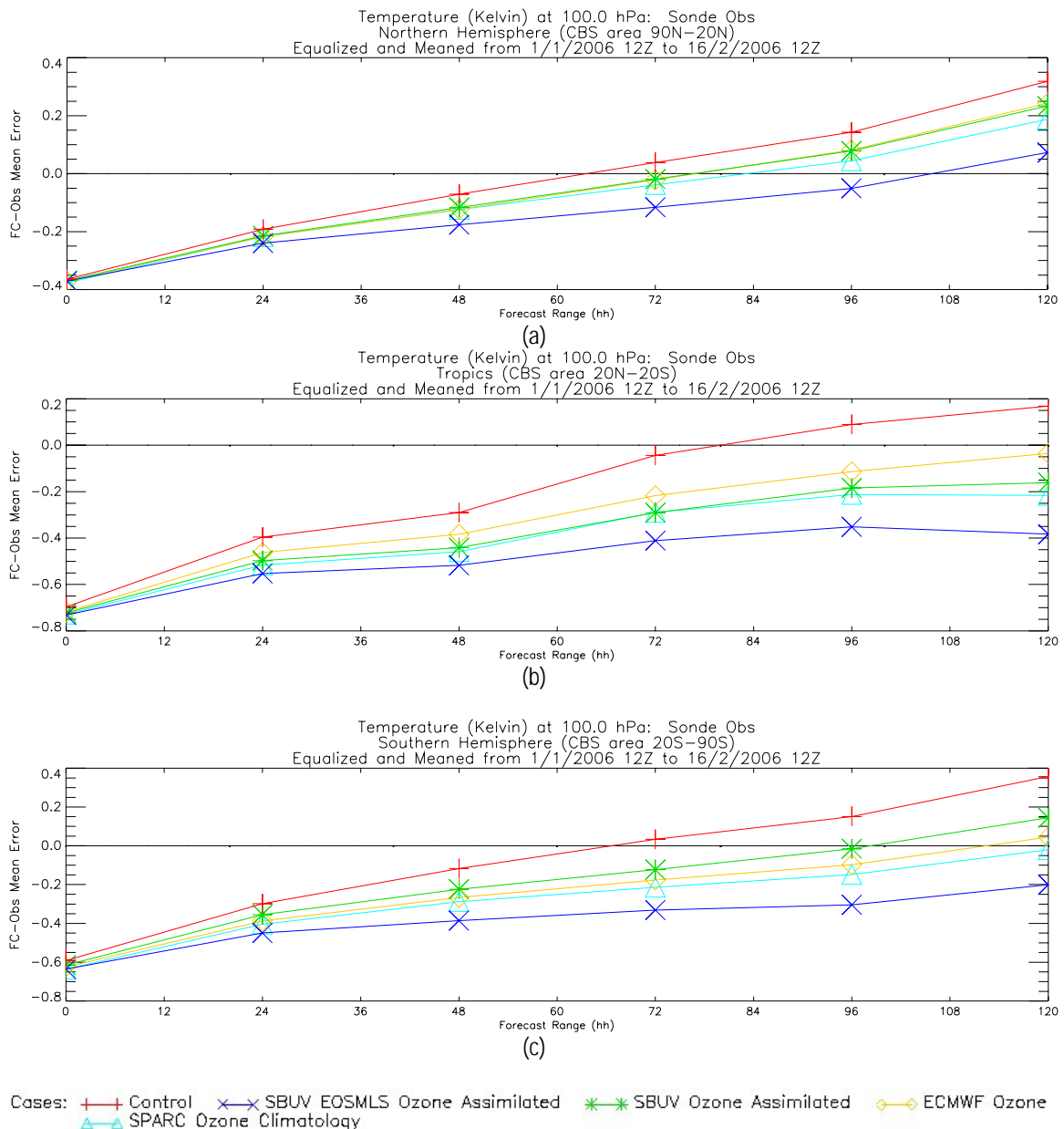


Figure 19 Plots of the change in mean error with forecast time. These plots illustrate the increase in the variability of the forecast –sonde mean errors with forecast time for each of the three regions. These plots are all for the 100hPa height. Plot a is the Northern hemisphere, plot b is the Tropics and plot c is the Southern hemisphere.

Figure 20 shows a time-series of the mean error for the Northern hemisphere at 850hPa T+24. Figure 21 shows a time series of the RMS error for the Tropics at 300hPa T+96. In each of these plots run ECMWF is clearly the outlier compared to the other experiments, this supports the global index and extended index results given in Section 3.1 and is consistent with Figure 16. These plots illustrate that run ECMWF is the outlier not only at analysis time but at several forecast times.

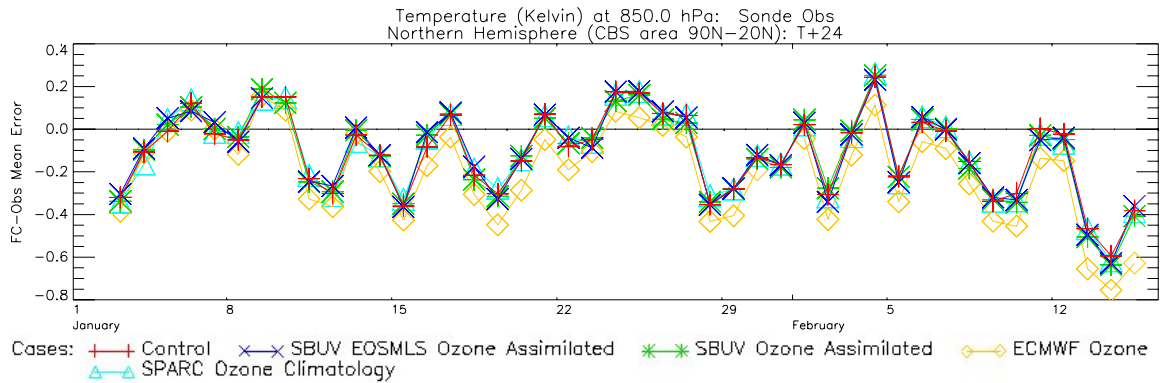


Figure 20 Time series of the forecast - observations mean error for the Northern hemisphere at 850hPa T+24

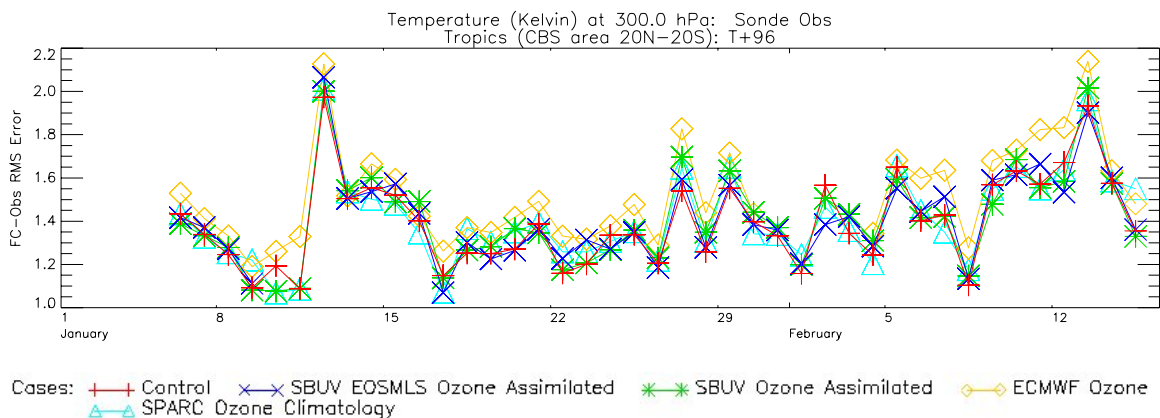


Figure 21 Time series of the forecast - observations RMS error for the Tropics at 300hPa T+96

In this section the temperature fields have been analysed using RMS and mean error statistics comparing the forecast to analysis and observations. In general run ECMWF showed the most significant differences from the other experiments, particularly evident in the time series plots shown in this section. There were few systematic differences between the experiments which made isolating the best method for changing ozone from this type of analysis more difficult.

## 4.0 Conclusions and future work

This document has presented four possible methods for improving the representation of ozone in the Unified Model. Four experiments have been run together with a control for an extended period which included a stratospheric warming in the Northern Hemisphere in 2006. The results presented have examined the impact of changing the ozone field on the Unified model.

The results presented here indicate that simply changing the ozone climatology used in the UM (run SPARC) can significantly improve the NWP index against analysis (+0.3) and slightly improve the index against observations (+0.05). The main benefit from using this climatology is the improvement seen in the Tropics; however the SPARC climatology is limited to troposphere and stratosphere and therefore does not have the same vertical extent as the Li and Shine climatology. The use of a combination of the SPARC climatology in the troposphere and stratosphere and Li and Shine climatology higher up would therefore be a more satisfactory way forward, particularly as the UM top level extends higher.

The results also provide a clear indication that the use of ECMWF ozone in the UM as an imported field actually causes a deterioration in the NWP index, possibly because the introduction of a field that is not consistent with the base model could cause imbalance in the evolution of the forecast. This may be a useful consideration if there is ever a proposal to use other ECMWF fields in the UM. In many situations, the distribution of errors from all the runs shows the run ECMWF error as an outlier. It is possible that these problems arise from the imported ECMWF ozone analyses being inconsistent with the forecast model transport, and thus the ozone field implied by that transport.

The global and extended index indicate that the 3D-Var system including the assimilation of ozone gives, for the period trialled, a consistently better performance than either climatology or ECMWF fields used in the UM. This was true even if only one observation type was assimilated. This is an important conclusion for the future work involving ozone. It should be noted however, that despite the NWP index showing obvious positive results from assimilating ozone the analysis shows no systematic reason for this improvement. Further investigation is necessary to establish exactly where the positive signal is coming from.

A further conclusion from this work is that in the upper stratosphere and above there are often large differences between forecast and analysis temperature fields, but the size of these differences often remain the same, even when the errors in the ozone field used are reduced. This suggests that there are inaccuracies in the calculation of radiative heating due to ozone at these levels. Thelen (2006) identified an overestimate of solar heating at these levels which could be addressed by upgrading the representation of ozone in the radiation scheme (specifically, this would require a re-calculation of the k-terms for ozone), although this would be time-consuming to do.

The next stage in assimilating ozone is to consider how ozone assimilation could be included in the current data assimilation system. There are a number of options for this and each will need to be considered to find the most efficient way of implementing ozone assimilation at the Met Office operationally. One option for future work is to upgrade the current 3D-Var ozone assimilation to 4D-Var and run it at every cycle, however this would be expensive to implement and it is possible that the computing resource may not currently stretch to this. Other options include running at fewer cycles or running the 3D-Var ozone assimilation within 4D-Var. Future work must therefore be focused on how ozone assimilation could be implemented to give the positive results demonstrated here without putting an added strain on computing resources.

## 5.0 References

Austin, J., Barwell, B.R., Cox, S.J., Hughes, P.A., Knight, J.R., Ross, G., Sinclair, P. and Webb, A.R., 1994, The diagnosis and forecast of clear sky ultraviolet levels at the Earth's surface, *Met Apps.*, 1, 321-336

Beekmann, M., Ancellet, G., Megie, G., Smit, H.G.J., and Kley, D., 1994, Intercomparison campaign for vertical ozone profiles including electrochemical sondes of ECC and Brewer-Mast type and a ground based UV-differential absorption radar, *J. Atmos. Chem.*, 19, 259-288

Cariolle, D and M. J. Deque, 1986. Southern Hemisphere medium-scale waves and total disturbances in a spectral circulation model. *J. Geophys. Res.* Vol. 91 Pages 10825 – 10884

Cariolle, D. and Morcrette, J.-J., 2006, A linearized approach to the radiative budget of the stratosphere: influence of the ozone distribution, *Geophys. Res. Lett.*, 33, L05806, doi:10.1029/2005GL025597

Davies et al., 2005. A new dynamical core for the Met Office's global and regional modelling of the atmosphere *Quarterly Journal of the Royal Meteorological Society*, Number 608, 04 2005 Part B, pp. 1759 - 1782(24).

EOSMLS web page 01<sup>st</sup> February 2007. <http://mls.jpl.nasa.gov/index-eos-mls.php>

Froidevaux, L et al, 2006, Early validation analyses of atmospheric profiles from EOSMLS on the Aura satellite, *IEEE Transactions on geoscience and remote sensing*, in press

Geer et al, 2006a, Assimilation of stratospheric ozone from MIPAS into a global general circulation model: the September 2002 vortex split, *Quart. J. Roy. Meteor. Soc.*, 132, 231-257

Geer et al, 2006b. The ASSET intercomparison of ozone analyses: method and first results. *Atmos. Chem Phys*, 6 5445 - 5474

Geer et al, 2007. Evaluation of linear ozone photochemistry parametrisations in a stratosphere-troposphere data assimilation system. *Atmos. Chem Phys.* , 7, 939-959

Haynes, P.H., 2005, Stratospheric Dynamics, *Annu. Rev. Fluid Mech.*, 37:263-293  
doi:10.1146/annurev.fluid/37.061903.175710

Jackson, D. and R. Saunders, 2002. Ozone Data Assimilation: Preliminary System. NWP Technical Report No. 394.

Jackson, D. 2004. Improvements in Ozone Data Assimilation at the Met Office. NWP Technical Report No. 454.

Jackson, D.R., 2007, Assimilation of EOSMLS ozone observations in the Met Office Data Assimilation System, *Quart. J. Roy. Met. Soc.*

Karoly, D., 2000 Stratospheric Aspects of Climate Forcing. SPARC newsletter No. 14  
[http://www.aero.jussieu.fr/~sparc/News14/14\\_Karoly.html](http://www.aero.jussieu.fr/~sparc/News14/14_Karoly.html)

Keil, M., D.R. Jackson and M. Holt (2007). The January 2006 low ozone event over the UK. *Atmos. Chem. Phys.*, 7, 961-972

Kerr, J.B., Fast, H., McElroy, C.T, Oltmans, S.J., Lathrop, J.A, Kyro, E., Paukkunen, A., Claude, H., Kohler, U., Sreedharan, C. R., Takao, T. and Tsukagoshi, Y., 1994, The 1991 WMO international ozonesonde intercomparison at Vanscoy, Canada, *Atmosphere Ocean*, 4, 685-716

Kiehl, J.T. *et al* (1999) Climate forcing due to tropospheric and stratospheric ozone. *J. Geophys. Res.* Vol. 104 No. D24 Pages 31239 – 31254

Komhyr, W.D, Barnes, R.A, Brothers, G.B, Lathrop, J.A, and Opperman, D.P, 1995, Electrochemical Concentration Cell ozonesonde performance evaluation during STOIC 1989, *J. Geophys. Res.*, 100, 9231-9244

Li, D. and K. P. Shine, A 4-Dimensional Ozone Climatology for UGAMP Models, UGAMP Internal Report No. 35, April 1995.

Livesey, N.J et al, 2005, EOSMLS, Version 1.5 Level 2 data quality and description document, JPL, California.

Lorenc, A. C., Ballard, S.P., Bell, R.S. et al, 2002, The Met. Office global three dimensional data assimilation scheme, *Quart. J. Roy. Meteor. Soc.*, 126, 2991-3012

Morcrette, J.-J., 2003, Ozone-radiation interactions in the ECMWF forecast system, ECMWF Technical Memo. 375

Randel, W. J., and F. Wu, 1999. A stratospheric ozone trends data set for global modelling studies. *Geophys. Res. Lett.*, 26, 3089-3092.

Smit, H. G. J., Strater, W., Helten, M., Kley, D., Ciupa, D., Claude, H. J., Kohler, U., Hoegger, B., Levrat, G., Johnson, B., Oltmans, S. J., Kerr, J. B., Tarasick, D. W., Davies, J., Shitamichi, M., Srivastav, S. K., Vialle, C. and Velghe, G., 1998, JOSIE: The 1996 WMO International intercomparison of ozonesondes under quasi flight conditions in the environmental simulation chamber at Julich, *Proceedings of the XVIII Quadrennial Ozone Symposium*, Eds R. Bojkov and G. Visconti, L'Aquila, Italy, September 1996

Thelen, J-C., 2006, Radiative aspects relating to the middle atmosphere model. Informal Met Office report. Available on request

Verification internal Met Office web page: Information available on request

Verification external Met Office web page: <http://www.metoffice.gov.uk/research/nwp/numerical/nwpindex.html> (As viewed on 28th March 2007)

Zhong, W. and Haigh, J.D., 2001, An efficient and accurate correlated-k parameterization of infrared radiative transfer for troposphere-stratosphere-mesosphere GCMs, *Atmos. Sci. Lett.*, 1, 125 - 135